mathematics

MDPI

Article

Hydrodynamic Impacts of Short Laser Pulses on Plasmas

Gaetano Fiore [1,2,*], Monica De Angelis [1], Renato Fedele [2,3], Gabriele Guerriero [1] and Dušan Jovanović [4,5]

[1] Department di Matematica e Applicazioni, Università di Napoli "Federico II", Complesso Universitario M. S. Angelo, Via Cintia, 80126 Napoli, Italy; modeange@unina.it (M.D.A.); gabriele.guerriero@unina.it (G.G.)
[2] INFN, Sezione di Napoli, Complesso MSA, Via Cintia, 80126 Napoli, Italy; renato.fedele@na.infn.it
[3] Department di Fisica, Università di Napoli "Federico II", Complesso Universitario M. S. Angelo, Via Cintia, 80126 Napoli, Italy
[4] Institute of Physics, University of Belgrade, 11080 Belgrade, Serbia; dusan.jovanovic@ipb.ac.rs
[5] Texas A & M University at Qatar, Doha 23874, Qatar
* Correspondence: gaetano.fiore@na.infn.it

Abstract: We determine conditions allowing for simplification of the description of the impact of a short and arbitrarily intense laser pulse onto a cold plasma at rest. If both the initial plasma density and pulse profile have plane symmetry, then suitable matched upper bounds on the maximum and the relative variations of the initial density, as well as on the intensity and duration of the pulse, ensure a strictly hydrodynamic evolution of the electron fluid without wave-breaking or vacuum-heating during its whole interaction with the pulse, while ions can be regarded as immobile. We use a recently developed fully relativistic plane model whereby the system of the Lorentz–Maxwell and continuity PDEs is reduced into a family of highly nonlinear but decoupled systems of non-autonomous Hamilton equations with one degree of freedom, the light-like coordinate $\xi = ct - z$ instead of time t as an independent variable, and new a priori estimates (eased by use of a Liapunov function) of the solutions in terms of the input data (i.e., the initial density and pulse profile). If the laser spot radius R is finite and is not too small, the same conclusions hold for the part of the plasma close to the axis $\vec{z}$ of cylindrical symmetry. These results may help in drastically simplifying the study of extreme acceleration mechanisms of electrons.

Keywords: plasma hydrodynamics; non-autonomous Hamilton equations; Liapunov function; relativistic electrodynamics; plasma wave; wave-breaking

MSC: 34C11; 34C99; 34C60; 76W05; 70H05; 70H40

Citation: Fiore, G.; De Angelis, M.; Fedele, R.; Guerriero, G.; Jovanović, D. Hydrodynamic Impacts of Short Laser Pulses on Plasmas. *Mathematics* **2022**, *10*, 2622. https://doi.org/10.3390/math10152622

Academic Editors: Vasily Novozhilov and Cunlu Zhao

Received: 17 June 2022
Accepted: 22 July 2022
Published: 27 July 2022

1. Introduction and Preliminaries

Laser–plasma interactions induced by ultra-intense laser pulses lead to a variety of very interesting phenomena [1–5], notably plasma compression for inertial fusion [6], laser wakefield acceleration (LWFA) [7–9] and other extremely compact acceleration mechanisms (e.g., hybrid laser-driven and particle-driven plasma wakefield acceleration [10]) of charged particles, which hopefully will be the basis of a generation of new table-top accelerators. This is paramount because accelerators have extremely important applications in particle physics, materials science, medicine, industry, environmental remediation, etc., and therefore huge investments (such as the EU-funded project *Eupraxia* [11–13]) are being developed all over the world to promote the development of such accelerators. Similar extreme conditions (huge electromagnetic fields and huge accelerations of charged particles in plasmas) occur in a number of violent astrophysical processes as well; see, e.g., [9] and references therein. In general, these phenomena are ruled by the equations of a kinetic theory coupled to Maxwell's equations, which can be only solved numerically via particle-in-cell (PIC) techniques. Unfortunately, PIC codes involve huge and expensive computations for each choice of the free parameters; even with the presently ever increasing computational power, exploring the parameter space blindly in order to single out interesting regions

remains prohibitively expensive. Sometimes, good predictions can be obtained by treating the plasma as a multicomponent fluid (electrons and ions) and by numerically solving the simpler associated hydrodynamic equations via multifluid codes such as QFluid [14] or hybrid kinetic/fluid codes. In general, however, it is not known a priori in which conditions or spacetime regions this is possible. Therefore any analytical insights that can simplify the work, at least in special cases or in a limited space-time region, are welcome.

This applies in particular to studying the impact of a very short (and possibly very intense) laser pulse perpendicularly onto a cold diluted plasma at rest, as well as onto matter which is locally ionized into a plasma by the front of the pulse itself. As is well known, electrons start oscillating orthogonally to the direction $\vec{z}$ of pulse propagation and drifting in the positive z-direction, pushed respectively by the electric and magnetic parts of the Lorentz force induced by the pulse; thereafter, electrons start oscillating longitudinally as well (i.e., in $\vec{z}$-direction), pushed by the restoring electric force induced by charge separation. Readers can find such initial longitudinal motions in Figure 1c and from the electron worldlines reported in Figures 7 and 8. It turns out that the initial dynamics are simpler if the pulse is *essentially short*. We say here (see Definition 1) that the pulse is *essentially short* if it overcomes each electron before the z-displacement, Δ, of the latter reaches a negative minimum for the first time; an essentially short pulse is *strictly short* if it overcomes each electron before Δ becomes negative for the first time. In other words, we regard a pulse as strictly short (essentially short) if it overcomes each electron before it finishes the first half (three quarters) longitudinal oscillation. In the nonrelativistic (NR) regime, a pulse which is symmetric under inversion around its center is strictly short (essentially short) if its duration l/c does not respectively exceed half (1) times the NR plasma oscillation period $t_H^{nr} \equiv \sqrt{\pi m/n_b e^2}$ associated with the maximum, n_b, of the initial electron density; that is (see Proposition 1), if

$$G_b := \sqrt{\frac{n_b e^2}{\pi m c^2}}\, l \;\leq\; \begin{cases} 1/2 \\ 1 \end{cases} \tag{1}$$

where $-e, m$ are the electron charge and mass c is the speed of light. (If the pulse is a slowly modulated monochromatic wave (58) with wavelength $\lambda = 2\pi/k$, this implies a fortiori $\frac{4\pi e^2}{mc^2} n_b \lambda^2 \ll 1$, meaning that the plasma is underdense). The general *relativistic* plasma oscillation period is not independent of the oscillation amplitude, but grows with the latter, which in turn grows with the pulse intensity. Correspondingly, Equation (16) can be fulfilled with a larger G_b; in addition, it is compatible with maximizing the oscillation amplitude, and thus the energy transfer from the pulse to the plasma wave, as for a given n_b and pulse energy such a maximization can be achieved [3,15] through a suitable

$$l \sim \tilde{\xi}_2, \qquad \text{(i.e., when } G_b \sim 1/2 \text{ in the nonrelativistic regime).} \tag{2}$$

We believe that such impacts require a deeper understanding because, among other things, they may generate: (i) a plasma wave (PW) [16,17] or even an *ion bubble* (a region containing only ions, because all electrons have been expelled out of it) [18–24] producing the LWFA, i.e., accelerating a small bunch of (socalled *witness*) electrons trailing the pulse at very high energy in the forward direction; and (ii) the *slingshot effect* [15,25,26], i.e., the backward acceleration and expulsion of energetic electrons from the vacuum–plasma interface during or just after the impact. The present work is one out of a few papers [27–29] arguing that, with the help of the plane, fully relativistic Lagrangian model of [30,31], and very little computational power, we can obtain important information about such an impact, in particular the formation of a PW, its persistence before wave-breaking (WB), and the features of the latter. As is known, a small WB is not necessarily undesirable, and may be used to produce and inject the mentioned witness electrons into the PW (*self-injection*).

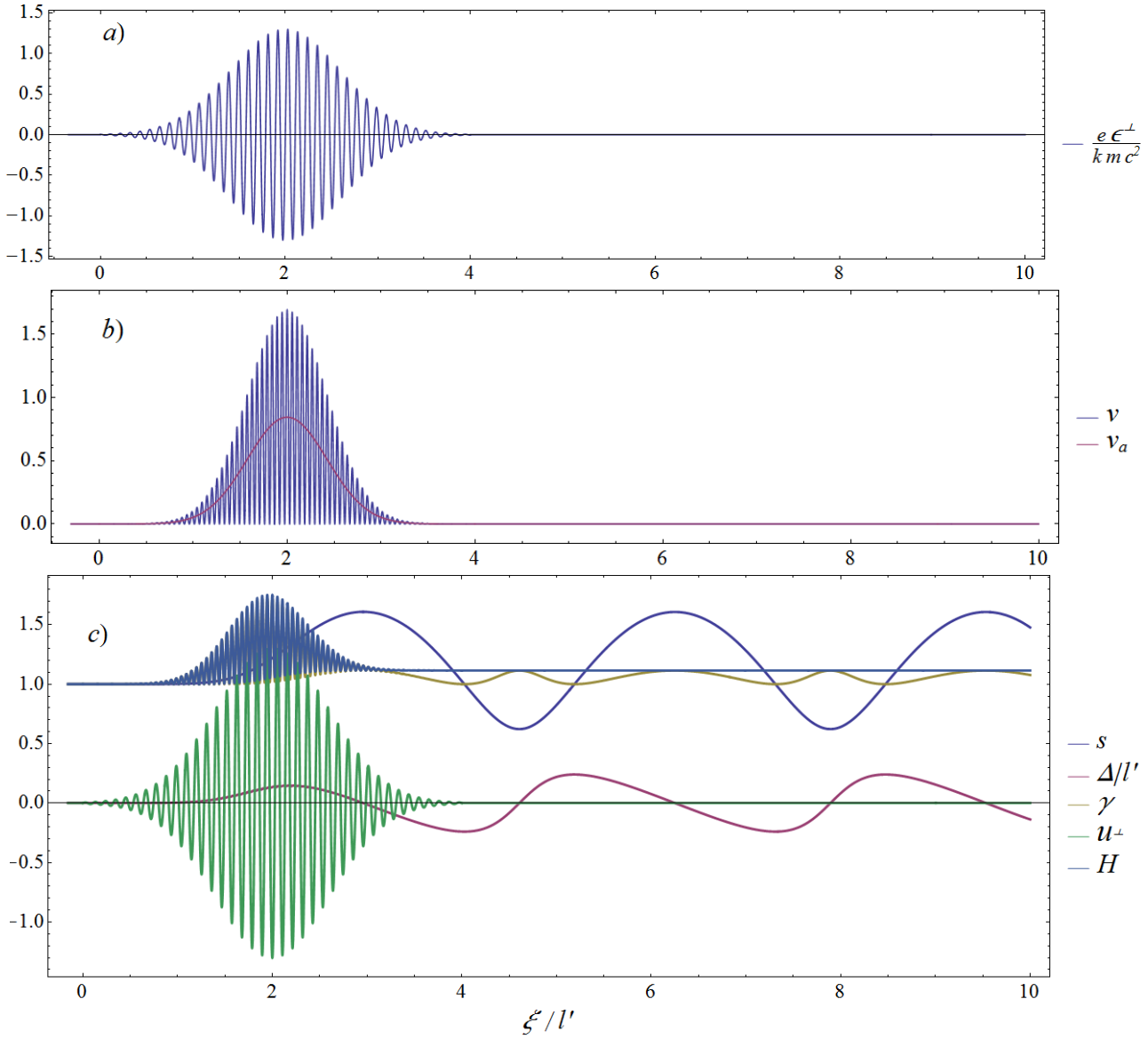

Figure 1. (**a**) Normalized amplitude of a linearly polarized (i.e., set $\psi = 0$ in (58)) monochromatic laser pulse slowly modulated by a Gaussian with *full width at half maximum* l' and peak amplitude $a_0 \equiv \lambda e E_M^{\perp}/mc^2 = 1.3$; this yields a moderately relativistic electron dynamics, and $\Delta_u \equiv \Delta^{(0)}(l) \simeq 0.45 l'$. If $l' = 7.5$ μm (corresponding to a pulse duration of $\tau' = l'/c \simeq 2.5 \times 10^{-14}$ s), and the wavelength is $\lambda = 0.8$ μm, then the corresponding peak intensity must be $I = 7.25 \times 10^{18}$ W/cm^2; these are typical values obtainable by Ti:Sapphire lasers in LWFA experiments. (**b**) The corresponding forcing term $v(\xi)$ and average-over-cycle (60) $v_a(\xi)$ of the latter. (**c**) Corresponding solution of (8) and (9), or equivalently of (14) if $Kn_0 l'^2 \simeq 4$; this value is obtained if $l' = 7.5$ μm and $\widetilde{n_0}(Z) \equiv n_0 = 2 \times 10^{18}$ cm^{-3} (a typical value of the electron density used in LWFA experiments). As expected, s is insensitive to the rapid oscillations of $\boldsymbol{\epsilon}^{\perp}$ for $\xi \in [0, l]$, while for $\xi \geq l$ the energy H is conserved and the solution is periodic. The length l is determined on physical grounds; if, e.g., the plasma is created locally by the impact of the pulse itself on a gas (e.g., hydrogen or helium), then $[0, l]$ has to contain all points ξ where the pulse intensity is sufficient to ionize the gas. Here, for simplicity and following convention, we have fixed it to be $l = 4l'$; the possible inaccuracy of such a cut is very small, because $\epsilon(0^+) = \epsilon(l^-)$ is 2^{-16} times the maximum $\epsilon(l/2)$ of the modulation, i.e., practically zero, which makes $G_b \equiv \sqrt{Kn_0}\, l \simeq 8$.

The plane model is as follows. We assume that the plasma is initially neutral, unmagnetized, and at rest, with zero densities in the region $z<0$. More precisely, the $t=0$ initial conditions for the electron fluid Eulerian density n_e and velocity $\boldsymbol{v}_e$ are of the type

$$\boldsymbol{v}_e(0,\boldsymbol{x}) = \boldsymbol{0}, \qquad n_e(0,\boldsymbol{x}) = \widetilde{n}_0(z), \tag{3}$$

where the initial electron (as well as proton) density $\widetilde{n}_0(z)$ fulfills

$$\widetilde{n}_0(z) = 0 \text{ if } z \le 0, \qquad 0 < \widetilde{n}_0(z) \le n_b \quad \text{if } z > 0 \tag{4}$$

for some $n_b > 0$ (a few examples are reported in Figure 2). Assuming that prior to the impact the laser pulse is a free plane transverse wave travelling in the z-direction, i.e., that the electric and magnetic fields $\boldsymbol{E}, \boldsymbol{B}$ are of the form

$$\boldsymbol{E}(t,\boldsymbol{x}) = \boldsymbol{E}^{\perp}(t,\boldsymbol{x}) = \boldsymbol{\epsilon}^{\perp}(ct-z), \qquad \boldsymbol{B} = \boldsymbol{B}^{\perp} = \mathbf{k}\times\boldsymbol{E}^{\perp} \qquad \text{if } t \le 0 \tag{5}$$

where $\boldsymbol{\epsilon}^{\perp}(\xi)$ has a bounded support with $\xi = 0$ as the left extreme (i.e., the pulse reaches the plasma at $t = 0$) and the superscript $\perp$ denotes vector components orthogonal to $\mathbf{k} \equiv \nabla z$. The input data of a specific problem are the functions $\widetilde{n}_0(z), \boldsymbol{\epsilon}^{\perp}(\xi)$; in addition, it is convenient to define the related functions

$$\boldsymbol{\alpha}^{\perp}(\xi) := -\int_{-\infty}^{\xi} d\zeta\, \boldsymbol{\epsilon}^{\perp}(\zeta), \qquad v(\xi) := \left[\frac{e\boldsymbol{\alpha}^{\perp}(\xi)}{mc^2}\right]^2, \tag{6}$$

$$\widetilde{N}(Z) := \int_0^Z d\zeta\, \widetilde{n}_0(\zeta), \qquad \mathcal{U}(\Delta; Z) := K\int_0^{\Delta} d\zeta\, (\Delta-\zeta)\, \widetilde{n}_0(Z+\zeta)\,, \tag{7}$$

where $K := \frac{4\pi e^2}{mc^2}$. By definition, v is dimensionless and nonnegative, and $\widetilde{N}(Z)$ strictly grows with Z. We can describe the plasma as a fully relativistic collisionless fluid of electrons and a static fluid of ions; as usual, in the short time lapse of interest here, the motion of the much heavier ions is negligible, with $\boldsymbol{E}, \boldsymbol{B}$ and the plasma dynamical variables fulfilling the Lorentz–Maxwell and continuity equations. As at the impact time $t = 0$ the plasma is made up of two static fluids, by continuity, such a hydrodynamical description (HD) is justified and we can neglect the depletion of the pulse at least for small $t > 0$; the specific time lapse is determined a posteriori by self-consistency. This allows us (see [30,31], or [32–35] for shorter presentations) to reduce the system of the Lorentz–Maxwell and continuity partial differential equations (PDEs) into ordinary ones, more precisely into the following continuous family of *decoupled Hamilton equations for systems with one degree of freedom*. Each system determines the complete Lagrangian (in the sense of non-Eulerian) description of the motion of the electrons having a same initial longitudinal coordinate $Z > 0$ (the *Z-electrons*, for brevity), and reads

$$\Delta'(\xi, Z) = \frac{1+v(\xi)}{2s^2(\xi, Z)} - \frac{1}{2}, \qquad s'(\xi, Z) = K\Big\{\widetilde{N}[Z+\Delta(\xi, Z)] - \widetilde{N}(Z)\Big\}; \tag{8}$$

it is equipped with the initial conditions

$$\Delta(0, Z) = 0, \qquad s(0, Z) = 1. \tag{9}$$

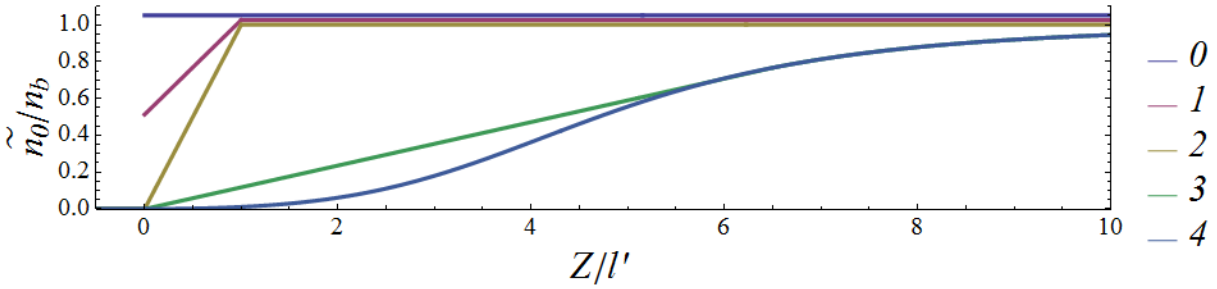

Figure 2. Plots of the ratios $\widetilde{n_0}/n_b$ for the following initial densities: (0) $\widetilde{n_0}(z) = n_b\,\theta(z)$. (1) $\widetilde{n_0}(z) = \frac{1}{2}n_b\,\theta(z)[1+\theta(l'-z)\,z/l'+\theta(z-l')]$. (2) $\widetilde{n_0}(z) = n_b\,[\theta(z)\,\theta(l'-z)\,z/l'+\theta(z-l')]$. (3) $\widetilde{n_0}(z) = n_b\left\{\frac{z}{\bar z}\,\frac{f(\bar z)}{1+f(\bar z)}\theta(z)\theta(\bar z-z)+\theta(z-\bar z)\,\frac{f(z)}{1+f(z)}\right\}$, where $f(z) := (0.1\,z/l')^2+(0.2\,z/l')^4$ and $\bar z = 6.5l'$; this grows as z for $z \le \bar z$ and coincides with the next one for $z > \bar z$. (4) $\widetilde{n_0}(z) = n_b\,\theta(z)\,\frac{f(z)}{1+f(z)}$.

Here, the unknown basic dynamical variables $\Delta(\xi,Z), s(\xi,Z)$ are respectivey the longitudinal displacement and s-factor of the Z-electrons espressed as functions of ξ, Z, while $z_e(\xi,Z) := Z+\Delta(\xi,Z)$ is the present longitudinal coordinate of the Z-electrons; s is the light-like component of the 4-velocity of the Z electrons, or equivalently is related to their 4-momentum by $p^0-cp^z \equiv mc^2 s$; it is positive-definite. In the NR regime $|s-1| \ll 1$; in the present fully relativistic regime, it need only satisfy the inequality $s > 0$. We consider all dynamical variables f (in the Lagrangian description) as functions of ξ, Z instead of t, Z; in the cited papers [30–35], the two dependences are denoted as $\hat f(\xi,Z)$ and $f(t,Z)$, respectively, although here we use only the former and thus denote it simply as $f(\xi,Z)$ without the $\hat{}$. In the above, f' stands for the total derivative $df/d\xi := \partial f/\partial\xi + s'\partial f/\partial s + \Delta'\partial f/\partial\Delta$ and Z plays the role of the family parameter; all of the other electron dynamical variables can be expressed in terms of Δ, s and the initial coordinates $\boldsymbol{X} \equiv (X,Y,Z)$ of the generic electron fluid element. In particular, in the basic approximation the dimensionless variable $\boldsymbol{u}^\perp := \boldsymbol{p}^\perp/mc$, i.e., the electrons' transverse momentum in mc units, is given by $\boldsymbol{u}^\perp = \frac{e\boldsymbol{A}^\perp}{mc^2}$; hence, $v = \boldsymbol{u}^{\perp 2}$. The light-like coordinate $\xi = ct-z$ in Minkowski spacetime can be adopted as an independent variable instead of time t, as all particles must travel at a speed lower than c; at the end, to express the solution as a function of t it is only necessary to replace ξ with the inverses $\tilde\xi(t,Z)$ of the strictly increasing (in ξ) functions $\hat t(\xi,Z) := (\xi+z_e(\xi,Z))/c$. Equation (8) consists of Hamilton equations, with $\xi, \Delta, -s$ playing the role of the usual t, q, p and the (dimensionless) Hamiltonian

$$H(\Delta,s,\xi;Z) \equiv \frac{s^2+1+v(\xi)}{2s} + \mathcal{U}(\Delta;Z); \tag{10}$$

the first term provides the kinetic + rest mass energy, while $\mathcal{U}$ plays the role of potential energy due to the electric charges' mutual interaction. Consequently, along the solutions of (8) $H' = \partial H/\partial\xi = v'/2s$. Integrating the latter identity by parts and using the definition (10) of H, we find

$$\frac{(s-1)^2}{2s} + \mathcal{U}(\Delta;Z) = H(\xi,Z) - 1 - \frac{v(\xi)}{2s(\xi,Z)} = \int_0^\xi d\eta\,\frac{vs'}{2s^2}(\eta,Z) =: \nu(\xi,Z). \tag{11}$$

The Hamilton Equations in (8) are non-autonomous for $0 < \xi < l$, where $[0,l]$ is the smallest closed interval containing the support of $\boldsymbol{\epsilon}^\perp$; ultra-intense pulses are characterized by $\max_{\xi\in[0,l]}\{v(\xi)\} \gg 1$ and induce ultra-relativistic electron motions. For $\xi \ge l$, (8) can be solved by quadrature as well, using the energy integrals of motion $H(\xi,Z) = H(l,Z) =: h(Z) = \text{const}$.

Solving (8) and (9) yields the motions of the Z-electrons' fluid elements, which are fully represented through their worldlines in Minkowski space. In Figures 7 and 8 we have displayed the projections onto the z, ct plane of these worldlines for two specific sets of input data; as can be seen, the PW emerges from them as a collective effect. Mathematically,

the PW features can be derived by reference to the Eulerian description of the electron fluid; the resulting flow is laminar, with xy plane symmetry. The Jacobian of the transformation $\boldsymbol{X} \mapsto \boldsymbol{x}_e \equiv (x_e, y_e, z_e)$ from the Lagrangian to the Eulerian coordinates reduces to $J(\xi, Z) = \partial z_e(\xi, Z)/\partial Z$, because $\boldsymbol{x}_e^{\perp} - \boldsymbol{X}^{\perp}$ does not depend on $\boldsymbol{X}^{\perp}$.

The HD breaks where worldlines intersect, leading to WB of the PW. No WB occurs as long as J remains positive. If the initial density is uniform, $\widetilde{n}_0(Z) = n_0 = \text{const}$, both Equation (8) and the initial conditions (9) become Z-independent, because (8 Right) takes the form $s' = M\Delta$, where $M := Kn_0$. Consequently, their solutions become Z-independent as well, and $J \equiv 1$ at all ξ. Otherwise, WB occurs after a sufficiently long time [36].

Our main goal here is to determine manageable sufficient conditions on $\widetilde{n}_0(z), \boldsymbol{\epsilon}^{\perp}(\xi)$ guaranteeing that $J(\xi, Z) > 0$ for all $Z > 0$ and $\xi \in [0, l]$, *without* solving the Cauchy problems (8) and (9). This ensures that there is no wave-breaking during the laser–plasma interaction (WBDLPI), i.e., while the Hamilton Equations (8) are non-autonomous (due to the dependence of v on ξ. We reach this goal by determining upper and lower bounds first on Δ, s, H (Section 2), then on J and $\partial s/\partial Z$ (Section 3), with the help of a suitable Liapunov function. These bounds provide useful approximations of these dynamical variables in the interval $0 \leq \xi \leq l$. As previously mentioned, the NR short-pulse conditions (1) are generalized by the ones (16) in the present fully relativistic regime. Inequalities (35) and (36) are respectively sufficient conditions for (16 Left) and (16 Right). Instead of (35), we can first check the stronger and more easily verifiable condition (40), or even the simplest and strongest one, $M_u l^2 \leq 2$. In the case that (36) is satisfied, we can exclude WBDLPI in the NR regime if (48) is fulfilled; in the general case, if one of the three conditions of Proposition 1 is fulfilled, namely if the plasma is initially sufficiently diluted and/or the local relative variations of its density are sufficiently small (if $Q_0 < 1$, the strongest and easiest to compute, is not fulfilled, $Q_1 < 1$ or $Q_2 < 1$ can be used). In Section 4 we compare the dynamics of s, Δ, J, σ induced by the same pulse on five representative $\widetilde{n}_0(z)$ having the same upper bound and asymptotic value n_b, both by numerically solving the equations and by applying the mentioned inequalities. In particular, we find that the density profile at the very edge of the plasma is critical; for instance, if $\widetilde{n}_0(z) \sim z$ as $z \to 0^+$, then WB occurs earlier than if $\widetilde{n}_0(z) \sim z^2$ or if $\lim_{z \to 0^+} \widetilde{n}_0(z) > 0$ (discontinuous density at $z = 0$), albeit with the electrons colliding at very small relative velocities. To produce LWFA, the laser pulse is usually fired orthogonally to a supersonic gas jet (e.g., hydrogen or helium); outside the jet nozzle it is $\widetilde{n}_0(z) \sim z^2$, and thus our results imply that such impacts occur in the hydrodynamic regime under rather broad conditions.

For $\xi \geq l$, by using the conservation of energy we can show [28] that, while Δ and s are periodic with a suitable period ξ_H, J and σ are *linearly quasiperiodic*, that is, they are of the form

$$f(\xi) = a(\xi) + \xi\, b(\xi), \qquad \xi \geq l, \tag{12}$$

where a, b are periodic in ξ with period ξ_H and b has zero average over a period; $b(\xi)$ oscillates between positive and negative values, as does the second term, which dominates as $\xi \to \infty$, with ξ acting as a modulating amplitude. Therefore, the occurrence of WB after the laser–plasma interaction is best investigated by studying the dependence (12) [28].

The spacetime region where the present plane hydrodynamic model predicting a laminar and xy-symmetric flow is self-consistent is determined (Section 4) by the conditions $J > 0$ (no collisions) and (62) (undepleted pulse approximation). For typical LWFA experiments, the length and time sizes allowed by (62) are respectively on the order of several hundred microns and femtoseconds, respectively. The spacetime region where the predictions of the model can be trusted is further reduced (Section 4) by the finite transverse size R of the laser pulse. According to our model, other phenomenal characteristic of plasma physics, such as turbulent flows, diffusion, heating, heat exchange, as well as the very motion of ions, can be excluded inside the latter region, although of course they can and will occur outside.

Finally, we point out that recent advances in multi-timescale analysis have permitted (semi)-analytical studies of laser–plasma interaction, including aspects of WB, in the ultrarelativistic regime using Vlasov description [37] .

2. A Priori Estimates of Δ, s, H for Small $\xi > 0$

The Cauchy problem (see (8) and (9)) is equivalent to the following integral one:

$$\Delta(\xi, Z) = \int_0^\xi d\eta \, \frac{1+v(\eta)}{2s^2(\eta, Z)} - \frac{\xi}{2}, \qquad s(\xi, Z) - 1 = \int_0^\xi d\eta \int_Z^{z_e(\eta,Z)} dZ' K\widetilde{n_0}(Z'). \tag{13}$$

If $\widetilde{n_0}(Z) \equiv n_0 = \text{const}$, then $\mathcal{U}(\Delta) = M\Delta^2/2$, $s' = M\Delta$, and (13) amounts to

$$s(\xi) = 1 + \frac{M}{2}\left[-\frac{\xi^2}{2} + \int_0^\xi d\eta \, (\xi - \eta)\frac{1+v}{s^2}(\eta)\right], \tag{14}$$

where $M := Kn_0$; once (14) is solved, we can obtain Δ from $\Delta = s'/M$. In Figure 1, we plot an example of a monochromatic laser pulse slowly modulated by a Gaussian along with the corresponding solution (s, Δ) in a constant density plasma; the qualitative behaviour of the solution remains the same if $\widetilde{n_0}(z) \neq \text{const}$. In the NR regime $v \ll 1$, whence $|\Delta/l| \ll 1$, $|\delta| \ll 1$, where $\delta := s - 1$; at lowest order in δ, Δ (8) and (9) reduce to the equations $\delta' = M\Delta$, $\Delta' = v/2 - \delta$ of a forced NR harmonic oscillator with trivial initial conditions. The solution is

$$\Delta(\xi) = \int_0^\xi d\eta \, \frac{v(\eta)}{2} \cos\left[\sqrt{M}(\xi - \eta)\right], \quad \delta(\xi) = \int_0^\xi d\eta \, \frac{v(\eta)}{2} \sin\left[\sqrt{M}(\xi - \eta)\right]. \tag{15}$$

By (8 Right), the zeroes of $\Delta(\cdot, Z)$ are extrema of $s(\cdot, Z)$ and vice versa, because $\widetilde{N}(Z)$ grows with Z. Let us recall how Δ, s start evolving from their initial values (9). As previously mentioned, for $\xi > 0$ all electrons reached by the pulse start to oscillate transversely and drift forward; in fact, $v(\xi)$ becomes positive, implying in turn that the right-hand side (rhs) of (8 Left) and Δ does as well; the $Z = 0$ electrons leave a layer of ions of finite thickness behind themselves that is completely evacuated of electrons. If the density vanished ($\widetilde{n_0} \equiv 0$), then we would obtain

$$s \equiv 1, \qquad \Delta(\xi, Z) = \int_0^\xi d\eta \, \frac{v(\eta)}{2} =: \Delta^{(0)}(\xi);$$

$\Delta^{(0)}(\xi)$ grows with ξ and is almost constant for $\xi > l$ if $v(\xi) \simeq 0$ for $\xi > l$ (which occurs if the pulse is slowly modulated (58)). On the contrary, as the density is positive, the growth of Δ implies the growth of the rhs of (8 Right), because the latter grows with Δ, as well as of $s(\xi, Z) - 1$. Meanwhile, $\Delta(\xi, Z)$ continues to grow as long as $1 + v(\xi) > s^2(\xi, Z)$, and reaches a maximum at $\tilde{\xi}_1(Z) \equiv$ the smallest $\xi > 0$ such that the rhs (8 Left) vanishes. $s(\xi, Z)$ keeps growing as long as $\Delta(\xi, Z) \geq 0$, reaches a maximum at the first zero $\tilde{\xi}_2 > \tilde{\xi}_1$ of $\Delta(\xi, Z)$, and decreases for $\xi > \tilde{\xi}_2$, while $\Delta(\xi, Z)$ is negative. $\Delta(\xi, Z)$ reaches a negative minimum at $\check{\xi}_3(Z) \equiv$ the smallest $\xi > \tilde{\xi}_2$, such that the rhs (8 Left) vanishes again. Here, we denote by $\tilde{\xi}_3(Z)$ the smallest $\xi > \check{\xi}_3$ such that $s(\xi, Z) = 1$ and $\mathcal{I} := [0, \tilde{\xi}_3]$. We encourage the reader to single out $\tilde{\xi}_1, \tilde{\xi}_2, \check{\xi}_3, \tilde{\xi}_3$ for the solution considered in Figure 1 from the graphs in 1c. If $\boldsymbol{\epsilon}^\perp$ is slowly modulated, then $v(l) \simeq 0$ (see Appendix A.2 for details, and Appendix 5.4 in [31] for further information); then, $\check{\xi}_3 \simeq \tilde{\xi}_3$ if $l < \check{\xi}_3$.

Definition 1. *A pulse is strictly short, essentially short with respect to $\widetilde{n_0}$ if it respectively fulfills*

$$\begin{cases} \Delta(\xi, Z) \geq 0\,, \\ s(\xi, Z) \geq 1\,, \end{cases} \quad \forall \xi \in [0, l],\ Z \geq 0 \qquad \Leftrightarrow \qquad l \leq \begin{cases} \tilde{\xi}_2(Z) \\ \tilde{\xi}_3(Z) \end{cases} \quad \forall Z \geq 0\,. \tag{16}$$

In the NR regime, if $\widetilde{n}_0(Z) \equiv n_0 = \text{const}$, these respectively amount to requiring that the corresponding solution (15) fulfills $\Delta(l) \geq 0$, $\delta(l) \geq 0$; if $\widetilde{n}_0(Z) \neq \text{const}$, it is sufficient to replace n_0 with n_b to obtain sufficient conditions for the fulfillment of (16), said conditions being

$$\begin{cases} 2\Delta(\xi) = \int_0^\xi d\eta\, v(\eta)\, \cos\left[\sqrt{Kn_b}(\xi-\eta)\right] \geq 0\,, \\ 2\delta(\xi) = \int_0^\xi d\eta\, v(\eta)\, \sin\left[\sqrt{Kn_b}(\xi-\eta)\right] \geq 0\,, \end{cases} \qquad \forall \xi \in [0, l]. \tag{17}$$

Proposition 1. *If v is symmetric about $\xi = l/2$, i.e., $v(\xi) = v(l-\xi)$, then (17 Left) amounts to $G_b \leq 1/2$; if in addition v has a unique maximum in $\xi = l/2$, then (17 Right) amounts to $G_b \leq 1$.*

The proof is provided in Appendix A.1. The assumption that $v(\xi)$ be symmetric is satisfied with very good approximation if the pulse is a slowly modulated one (58) with a symmetric modulation $\epsilon(\xi)$ about $\xi = l/2$ (as in Figure 1b), per (59).

The following estimates hold for $\xi \in \mathcal{I} = [0, \tilde{\xi}_3]$. First, $s \geq 1$ and (13 Left) imply the bound

$$\Delta(\xi, Z) \leq \Delta^{(0)}(\xi). \tag{18}$$

2.1. Constant Density Case

If $\widetilde{n}_0(Z) \equiv n_0 > 0$, for $\xi \in \mathcal{I}$ we find by (18) $s(\xi) - 1 = M \int_0^\xi d\eta\, \Delta(\eta) \leq M \int_0^\xi d\eta\, \Delta^{(0)}(\eta)$, i.e.,

$$s(\xi) \leq 1 + \frac{M}{2} \int_0^\xi d\eta\, (\xi - \eta)\, v(\eta) =: s^{(1)}(\xi). \tag{19}$$

As $s^{(1)}(\xi)$ grows strictly with ξ and is convex, Equation (19) and (13 Left) in turn imply

$$\Delta(\xi) \quad \geq \quad \int_0^\xi d\eta\, \frac{1+v(\eta)}{2[s^{(1)}(\eta)]^2} - \frac{\xi}{2} =: \Delta^{(1)}(\xi). \tag{20}$$

It is apparent that $\Delta^{(1)}(\xi)$ vanishes at $\xi = 0$ and grows with ξ for small $\xi > 0$ until its (unique) maximum point, while for larger ξ it decreases and becomes negative. Hence, a lower bound $\tilde{\xi}_2^{(1)}$ for $\tilde{\xi}_2$ is the smallest $\xi > 0$ such that $\Delta^{(1)}(\xi) = 0$. Therefore, $\Delta^{(1)}(l) \geq 0$ ensures that $\tilde{\xi}_2 \geq \tilde{\xi}_2^{(1)} \geq l$.

Equation (13 Right) implies that $s(\xi) - 1 = M \int_0^\xi d\eta\, \Delta(\eta) \geq M \int_0^\xi d\eta\, \Delta^{(1)}(\eta)$, namely,

$$\frac{M}{2} f(\xi) =: s^{(2)}(\xi), \qquad f(\xi) := \int_0^\xi d\eta\, \frac{(\xi-\eta)[1+v(\eta)]}{[s^{(1)}(\eta)]^2} - \frac{\xi^2}{2}. \tag{21}$$

At least for small ξ, this is a more stringent lower bound for s in $\mathcal{I}$ than $s \geq 1$; $f(\xi)$ vanishes at $\xi = 0$, and grows with ξ for small $\xi > 0$ until its (unique) maximum point; for larger ξ, it decreases and becomes negative. Hence, a lower bound $\tilde{\xi}_3^{(1)}$ for $\tilde{\xi}_3$ is the smallest $\xi > 0$ such that $f(\xi) = 0$. Therefore, $f(l) \geq 0$ ensures that $\tilde{\xi}_3 \geq \tilde{\xi}_3^{(1)} \geq l$.

2.2. Generic Density Case

Let $\check{n}(\xi, Z) := \widetilde{n}_0\left[z_e(\xi, Z)\right]$, $\tilde{\xi}_2' := \min\{\tilde{\xi}_2, l\}$, $n_u, n_d > 0$ be some upper, lower bounds on $\check{n}$

$$n_d(Z) \leq \check{n}(\xi, Z) \leq n_u(Z) \tag{22}$$

for $0 \leq \xi \leq \tilde{\xi}_2'$. If $\widetilde{n}_0(Z) \equiv n_0$, then $\check{n} \equiv n_0$, and we can set $n_u = n_d = n_0$. In general, a Z-independent choice of n_u is $n_u = n_b$; see (4). More accurately, with $\Delta_u > 0$ such that

$$\Delta(\xi, Z) \leq \Delta_u \qquad \forall \xi \in [0, \tilde{\xi}_3], \tag{23}$$

then $0 \le \Delta(\xi, Z) \le \Delta_u(Z)$ for all $\xi \in [0, \tilde{\xi}_2]$ (by the definition of $\tilde{\xi}_2$), and (22) holds, choosing

$$n_u(Z) = \max_{Z' \in [Z, Z+\Delta_u]} \{\widetilde{n}_0(Z')\}, \qquad n_d(Z) = \min_{Z' \in [Z, Z+\Delta_u]} \{\widetilde{n}_0(Z')\}; \tag{24}$$

in general, (24 Left) is a lower (and therefore better) upper bound than $n_u = n_b$. Henceforth we abbreviate $M_u(Z) := Kn_u(Z)$, $M_d(Z) := Kn_d(Z)$. By (18), we can adopt the simple choice $\Delta_u := \Delta^{(0)}(l)$ (if $v(l) \simeq 0$, as occurs if the pulse is a slowly modulated one (58), then $\Delta^{(0)}(\xi) \simeq \Delta^{(0)}(l)$ if $\xi > l$, and (22) holds with $\Delta_u = \Delta^{(0)}(l)$ for all $0 \le \xi \le \tilde{\xi}_2$ even if $\tilde{\xi}_2 > l$).

Lemma 1. *For all $\xi \in [0, \tilde{\xi}_3]$, the rhs ν of (11) can be bound by*

$$\nu(\xi, Z) \le \nu_u(\xi, Z) := \frac{M_u(Z)}{2} \left[\Delta^{(0)}(\xi)\right]^2 \tag{25}$$

Proof. For $\xi \in [0, \tilde{\xi}_2]$, the inequality is proven as follows:

$$\nu(\xi) = \int_0^\xi d\eta \, \frac{vs'}{2s^2}(\eta) \le \int_0^\xi d\eta \, \frac{v}{2s^2}(\eta) \int_Z^{Z+\Delta(\eta)} dz \, M_u = M_u \int_0^\xi d\eta \, \frac{v\Delta}{2s^2}(\eta) \le M_u \int_0^\xi d\eta \, \frac{v\Delta^{(0)}}{2}(\eta) = \nu_u(\xi)$$

using $\Delta^{(0)\prime} = v/2$; for brevity, we have not displayed the Z argument here. The inequality holds in $]\tilde{\xi}_2, \tilde{\xi}_3]$ as well, because there ν decreases, whereas ν_u grows. □

The maximum of $\nu(\xi, Z)$ in $[0, \tilde{\xi}_3]$ is in $\xi = \tilde{\xi}_2$ because $s' > 0$ in $]0, \tilde{\xi}_2[$ and $s' < 0$ in $]\tilde{\xi}_2, \tilde{\xi}_3[$. To obtain upper, lower bounds s_u, s_d for $s(\xi, Z)$ and a lower bound $\Delta_d(Z)$ for $\Delta(\xi, Z)$ in the longer interval $0 \le \xi \le \tilde{\xi}_3' := \min\{l, \tilde{\xi}_3\}$, we use (25) to majorize

$$\nu(\xi, Z) \le \nu(\tilde{\xi}_2, Z) \le \frac{M_u}{2} \left[\Delta^{(0)}(\tilde{\xi}_2)\right]^2 \le \frac{M_u}{2} \Delta_u^2$$

(again, if $v(l) \simeq 0$, as occurs if the pulse is a slowly modulated one (58), then $\Delta^{(0)}(\xi) \simeq \Delta^{(0)}(l)$ if $\xi > l$, and these results remain valid if we replace $\tilde{\xi}_3'$ by $\tilde{\xi}_3$, even if $\tilde{\xi}_3 > l$).

When replaced in (11), this yields $(s-1)^2/2s \le M_u \Delta_u^2/2$ and $\mathcal{U} \le M_u \Delta_u^2/2$, whence

$$s_d \le s(\xi, Z) \le s_u, \quad \left.\begin{matrix} s_u \\ s_d \end{matrix}\right\} := 1 + \frac{M_u}{2}\Delta_u^2 \pm \sqrt{\left(1 + \frac{M_u}{2}\Delta_u^2\right)^2 - 1}, \qquad \Delta(\xi, Z) \ge \Delta_d(Z), \tag{26}$$

where Δ_d is the negative solution of the equation $\mathcal{U}(\Delta; Z) = M_u(Z)\Delta_u^2/2$ (as a first estimate, $\Delta_d = -\Delta_u$). Clearly, $1/s_d = s_u > 1$.

Proposition 2. *For all $\xi \in [0, \tilde{\xi}_3']$, the dynamical variables Δ, s are bounded as follows:*

$$\begin{aligned} &\Delta^{(0)}(\xi, Z) \ge \Delta(\xi, Z) \ge \Delta^{(1)}(\xi, Z), \\ &s^{(1)}(\xi, Z) \ge s(\xi, Z) \ge s^{(2)}(\xi, Z), \end{aligned} \tag{27}$$

where $\Delta^{(0)}(\xi) := \int_0^\xi d\eta\, v(\eta)/2$, *and*

$$
\begin{aligned}
&s^{(1)}(\xi,Z) := \min\{s_u, 1+g(\xi,Z)\}, \quad g(\xi,Z) := \frac{M_u}{2}\int_0^\xi d\eta\,(\xi-\eta)\,v(\eta),\\
&\Delta^{(1)}(\xi,Z) := \max\{\Delta_d, d(\xi,Z)\}, \quad d(\xi,Z) := \int_0^\xi d\eta\,\frac{1+v(\eta)}{2[s^{(1)}(\eta,Z)]^2} - \frac{\xi}{2},\\
&s^{(2)}(\xi,Z) := \begin{cases} 1+\frac{M_d}{2}f(\xi,Z) & 0 \le \xi \le \tilde\xi_2^{(1)} \\ \max\left\{s_d, 1+\left[\frac{M_d}{2}-\frac{M_u'}{2}\right]f\left(\tilde\xi_2^{(1)},Z\right)+\frac{M_u'}{2}f(\xi,Z)\right\} & \tilde\xi_2^{(1)} < \xi \le \tilde\xi_3', \end{cases}\\
&f(\xi,Z) := \int_0^\xi d\eta\,(\xi-\eta)\left\{\frac{1+v(\eta)}{[s^{(1)}(\eta,Z)]^2}-1\right\},
\end{aligned}
\tag{28}
$$

where $\tilde\xi_2^{(1)}(Z) < \tilde\xi_2$ *is the zero of* $d(\xi,Z)$ *as well as the maximum point of* $f(\xi,Z)$, *and* $M_u'/K = n_u' := \max_{Z'\in[Z+\Delta_d,Z]}\{\tilde n_0(Z')\}$. *Moreover, the value of the Hamiltonian is bounded by*

$$
H_d := 1+\frac{v}{2s^{(1)}}+\nu_d \;\le\; H \;\le\; 1+\frac{v}{2s^{(2)}}+\frac{M_u}{2}\left[\Delta^{(0)}\right]^2 =: H_u,
\tag{29}
$$

where, dubbing the maximum of $d(\xi,Z)$ *by* $\tilde\xi_1^{(1)}(Z)$, *we have defined*

$$
\nu_d(\xi,Z) := \begin{cases} \frac{M_d(Z)}{2}\left[\Delta^{(1)}(\xi,Z)\right]^2 & \xi \in \left[0,\tilde\xi_1^{(1)}\right], \\ \frac{M_d(Z)}{2}\left[\Delta^{(1)}\left(\tilde\xi_1^{(1)}\right)\right]^2 & \xi \in \left[\tilde\xi_1^{(1)},\tilde\xi_2^{(1)}\right], \\ \frac{M_d(Z)}{2}\left[\Delta^{(1)}\left(\tilde\xi_1^{(1)},Z\right)\right]^2 + M_u'(Z)\int_{\tilde\xi_2^{(1)}}^\xi d\eta\,\frac{v\Delta^{(1)}}{2}(\eta,Z) & \xi \in \left[\tilde\xi_2^{(1)},\tilde\xi_3'\right]. \end{cases}
\tag{30}
$$

Note that $\tilde\xi_1^{(1)}(Z) < \tilde\xi_1(Z)$. Equations (27) and (28) reduce to (18) and (21) if $\tilde n_0(Z) \equiv n_0 = \text{const}$.

Proof. The left inequality in (27 Left) is the already proven (18). Equation (13) by (24), (18) implies $s(\xi,Z) - 1 \le \int_0^\xi d\eta\, M_u \Delta(\eta,Z) \le M_u \int_0^\xi d\eta\,\Delta^{(0)}(\eta)$, which together with (26 Left) implies the left inequality in (27 Right); the latter, together with (13 Left), (26 Right), in turn implies the right inequality in (27 Left). First, $d(\xi,Z) = f'(\xi,Z)$ vanishes at $\xi = 0$, grows with ξ for small $\xi > 0$ until it reaches a maximum for sufficiently large ξ, then decreases to negative values. Hence, $\tilde\xi_2^{(1)}$, i.e., the smallest $\xi > 0$ such that $\Delta^{(1)}(\xi,Z) = 0$, is indeed a lower bound for $\tilde\xi_2$; meanwhile, $\tilde\xi_2^{(1)}$ is the maximum point of f and $s^{(2)}$. Equation (13) implies that for all $\xi \in [0,\tilde\xi_2]$

$$
s(\xi,Z)-1 \ge M_d\int_0^\xi d\eta\,\Delta(\eta,Z) \ge M_d\int_0^\xi d\eta\, d(\eta,Z) = \frac{M_d}{2}f(\xi,Z).
\tag{31}
$$

If $\xi \in]\tilde\xi_2,\tilde\xi_3']$, integrating (8 Right) over $[\tilde\xi_2,\xi]$ and recalling that $\Delta_d \le \Delta < 0$ there, we find

$$
\begin{aligned}
s(\xi,Z)-s(\tilde\xi_2,Z) &= -K\int_{\tilde\xi_2}^\xi d\eta \int_{Z+\Delta(\eta Z)}^Z dZ'\,\tilde n_0(Z') \ge M_u'\int_{\tilde\xi_2}^\xi d\eta\,\Delta(\eta,Z) \ge M_u'\int_{\tilde\xi_2}^\xi d\eta\,\Delta^{(1)}(\eta,Z)\\
&> M_u'\int_{\tilde\xi_2^{(1)}}^\xi d\eta\,\Delta^{(1)}(\eta,Z) \ge \frac{M_u'}{2}\left[f(\xi,Z)-f\left(\tilde\xi_2^{(1)},Z\right)\right]
\end{aligned}
\tag{32}
$$

where the first inequality in the last line holds because $\Delta^{(1)}(\eta,Z) < 0$ if $\eta \in [\tilde{\xi}_2^{(1)}, \tilde{\xi}_2]$; as s has its maximum in $\tilde{\xi}_2$, (31) implies in particular that $s(\tilde{\xi}_2,Z) \geq s(\tilde{\xi}_2^{(1)},Z) \geq 1+\frac{M_d}{2} f(\tilde{\xi}_2^{(1)},Z)$, which when replaced in (32) provides

$$s(\xi,Z) \geq 1+\frac{M_d}{2} f(\tilde{\xi}_2^{(1)},Z) + \frac{M'_u}{2}\left[f(\xi,Z) - f\left(\tilde{\xi}_2^{(1)},Z\right)\right];$$

the latter inequality and (31) amount to the right inequality in (27 Right), which holds, together with $s(\xi,Z) \geq 1$. The right inequality in (29) follows from (11) and (25). From $2\Delta^{(1)\prime} = (1+v)/s^{(1)2} - 1 \leq v/s^{(1)2}$, it follows for $\xi \in [0,\tilde{\xi}_2]$ that

$$v(\xi,Z) \geq M_d \int_0^\xi d\eta \, \frac{v\Delta}{2s^2}(\eta) \geq M_d \int_0^\xi d\eta \, \frac{v\Delta^{(1)}}{2s^{(1)2}}(\eta) \geq M_d \int_0^\xi d\eta \left[\Delta^{(1)}\Delta^{(1)\prime}\right](\eta) = \frac{M_d}{2}\left[\Delta^{(1)}(\xi)\right]^2,$$

where again, for brevity, we have not displayed the Z argument. As the rhs has its maximum in $\xi = \tilde{\xi}_1^{(1)}$, whereas $v(\xi,Z)$ can grow in $[\tilde{\xi}_1^{(1)}, \tilde{\xi}_2]$, we obtain

$$v(\xi,Z) \geq \begin{cases} \frac{M_d}{2}\left[\Delta^{(1)}(\xi)\right]^2 & \xi \in [0,\tilde{\xi}_1^{(1)}] \\ \frac{M_d}{2}\left[\Delta^{(1)}(\tilde{\xi}_1^{(1)})\right]^2 & \xi \in [\tilde{\xi}_1^{(1)}, \tilde{\xi}_2] \end{cases} \tag{33}$$

If $\xi \in [\tilde{\xi}_2, \tilde{\xi}'_3]$, then $s', \Delta < 0$ in $[\tilde{\xi}_2, \xi]$, and

$$\int_{\tilde{\xi}_2}^\xi d\eta \, \frac{vs'}{2s^2}(\eta) = -\int_{\tilde{\xi}_2}^\xi d\eta \, \frac{Kv}{2s^2}(\eta) \int_{Z+\Delta(\eta)}^Z dz \, \widetilde{n}_0(z) \geq M'_u \int_{\tilde{\xi}_2}^\xi d\eta \, \frac{v\Delta}{2}(\eta) \geq M'_u \int_{\tilde{\xi}_2}^\xi d\eta \, \frac{v\Delta^{(1)}}{2}(\eta) > M'_u \int_{\tilde{\xi}_2^{(1)}}^\xi d\eta \, \frac{v\Delta^{(1)}}{2}(\eta)$$

where the last inequality holds because $\Delta^{(1)} < 0$ in $[\tilde{\xi}_2^{(1)}, \tilde{\xi}_2]$; by summing this inequality and $v(\tilde{\xi}_2,Z) \geq M_d\left[\Delta^{(1)}(\tilde{\xi}_1^{(1)})\right]^2/2$ we obtain $v(\xi,Z) \geq M_d\left[\Delta^{(1)}(\tilde{\xi}_1^{(1)})\right]^2/2 + M'_u \int_{\tilde{\xi}_2^{(1)}}^\xi d\eta \, v\Delta^{(1)}(\eta)/2$, which actually holds for all $\xi \in]\tilde{\xi}_2^{(1)}, \tilde{\xi}'_3]$ by (33) and because the second term is negative if $\xi \in [\tilde{\xi}_2^{(1)}, \tilde{\xi}_2]$. Summing up, we find $v(\xi,Z) \geq v_d(\xi,Z)$ in all the interval $[0,\tilde{\xi}'_3]$; this, together with (11), implies the left inequality (29). □

By (26), inequalities (22) hold for all $\xi \in [0,\tilde{\xi}'_3]$ if, rather than by (24), we define n_u, n_d by

$$n_u(Z) = \max_{Z' \in \left[Z+\Delta_d, Z+\Delta_u\right]} \{\widetilde{n}_0(Z')\}, \qquad n_d(Z) = \min_{Z' \in \left[Z+\Delta_d, Z+\Delta_u\right]} \{\widetilde{n}_0(Z')\}. \tag{34}$$

As mentioned previously, $\Delta^{(1)}(\xi,Z) = d(\xi,Z) = f'(\xi,Z)$ vanishes at $\xi = 0$, grows up to its unique positive maximum at $\tilde{\xi}_1^{(1)}$, then decreases to negative values; $\tilde{\xi}_2^{(1)}$ is the unique $\xi > \tilde{\xi}_1^{(1)}$ such that $\Delta^{(1)}(\xi,Z) = 0$. Hence, $\tilde{\xi}_2^{(1)}$ is a lower bound for $\tilde{\xi}_2$. Therefore, the condition

$$\Delta^{(1)}(l,Z) \geq 0 \tag{35}$$

ensures that $\tilde{\xi}_2(Z) \geq \tilde{\xi}_2^{(1)}(Z) \geq l$, namely, that the pulse is strictly short. Similarly, $s^{(2)} - 1$ vanishes at $\xi = 0$, grows up to its unique positive positive maximum at $\tilde{\xi}_2^{(1)}$, then decreases to negative values. Hence, a lower bound $\tilde{\xi}_3^{(1)}$ for $\tilde{\xi}_3$ is the unique $\xi > \tilde{\xi}_2^{(1)}$ such that $s^{(2)}(\xi,Z) = 1$, and the condition

$$s^{(2)}(l,Z) \geq 1 \tag{36}$$

ensures that $\tilde{\xi}_3(Z) \geq \tilde{\xi}_3^{(1)}(Z) \geq l \equiv \tilde{\xi}_3'$, namely, that the pulse is essentially short. Moreover, with this assumption we find by (29) the following upper and lower bounds on the final Z-electron energy $h(Z)$ after their interaction with the pulse:

$$H_d(l,Z) \;\leq\; h(Z) \;\leq\; H_u(l,Z). \tag{37}$$

In Figures 3 and 4, we plot $s(\cdot,Z), \Delta(\cdot,Z)$ for two values of Z and the associated upper and lower bounds corresponding to the densities of Figure 2, which have the same asymptotic value n_b. As can be seen, the bounds agree well. Moreover, a useful lower bound for $\Delta^{(1)}$ is provided by the following lemma.

Lemma 2.

$$\Delta^{(1)}(\xi,Z) \geq \Delta^{(0)}(\xi)\left[1 - \frac{M_u(Z)}{2}\xi^2 - M_u(Z)\,\xi\,\Delta^{(0)}(\xi)\right]. \tag{38}$$

Proof. $g \geq 0$ implies $1/(1+g) \geq 1-g$, $1/(1+g)^2 \geq (1-g)^2 \geq 1-2g$ such that

$$2\Delta^{(1)}(\xi,Z) \geq \int_0^\xi d\eta\,\{[1+v(\eta)][1-2g(\eta,Z)]-1\} = 2\Delta^{(0)}(\xi) - \int_0^\xi d\eta\,2g(\eta,Z)[1+v(\eta)]. \tag{39}$$

The definitions of $g, \Delta^{(0)}$ immediately imply the inequality $g(\xi,Z) \leq M_u\xi\Delta^{(0)}(\xi)$, whence

$$\int_0^\xi d\eta\,2g(\eta,Z) \leq M_u\int_0^\xi d\eta\,\eta 2\Delta^{(0)}(\eta) \leq M_u\int_0^\xi d\eta\,\eta 2\Delta^{(0)}(\xi) \leq M_u\xi^2\Delta^{(0)}(\xi),$$

$$\int_0^\xi d\eta\,2g(\eta,Z)v(\eta) \leq M_u\int_0^\xi d\eta\,\eta 2\Delta^{(0)}(\eta)v(\eta) \leq M_u\int_0^\xi d\eta\,\xi 4\left[\Delta^{(0)}\Delta^{(0)\prime}\right](\eta) = 2M_u\xi[\Delta^{(0)}(\xi)]^2$$

Replacing the latter in (39), we obtain (38). □

As a consequence, if the square bracket at the rhs (38) is nonnegative, then is as well $\Delta^{(1)}(\xi,Z)$, and therefore another condition ensuring that $\tilde{\xi}_2 > l$ (i.e., that the pulse is strictly short) is

$$M_u(Z)\,l^2\left[1 + 2\frac{\Delta_u}{l}\right] \leq 2, \tag{40}$$

which is more easily computable, although more difficult to satisfy, than (35).

More stringent (though less easily computable) bounds than (27) could be found by replacing them in (13) and reiterating the previous arguments. The first step is the new bound $\Delta(\xi,Z) \leq \Delta^{(2)}(\xi,Z) := \int_0^\xi d\eta\,\frac{1+v(\eta)}{2\left[s^{(2)}(\eta,Z)\right]^2} - \frac{\xi}{2}$, the second is setting $\Delta_u := \max_{\xi\in[0,l]}\{\Delta^{(2)}(\xi)\}$ instead of $\Delta_u := \Delta^{(0)}(l)$ in (24), etc. However, for the scope of the present work we content ourselves with these basic relations.

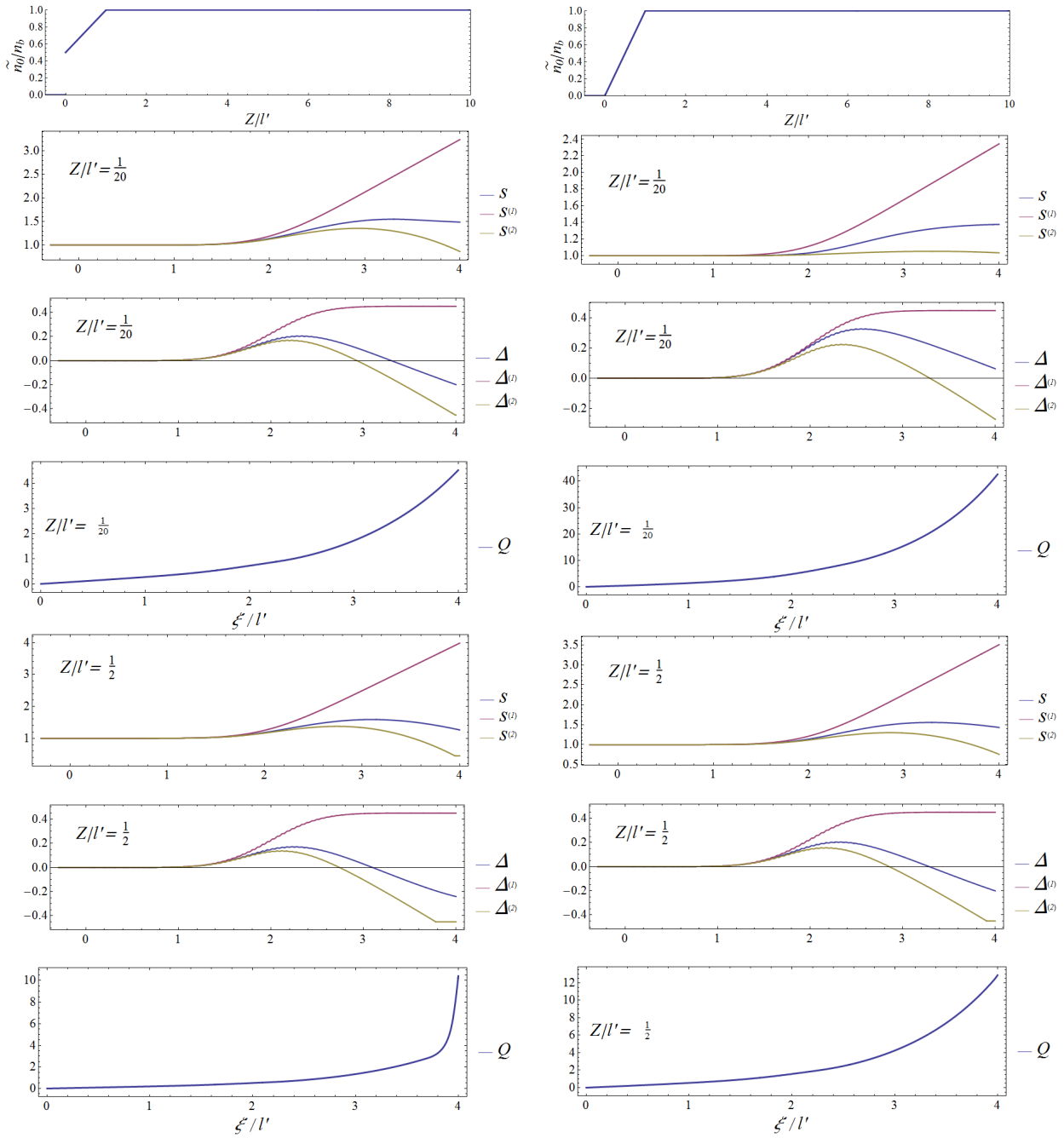

Figure 3. The initial electron densities (1), (2) of Figure 2 (first line; left and right, respectively). Below, assuming $n_b = 2 \times 10^{18}\text{cm}^{-3}$, we plot the corresponding s, Δ, their upper and lower bounds $s^{(1)}, s^{(2)}, \Delta^{(1)}, \Delta^{(2)}$, and the function Q, vs. ξ during interaction with the pulse in Figure 1 for the same sample values, $Z = l'/20$ and $Z = l'/2$ of Z. The values $Q_2(Z) := Q(l,Z)$ can be read off the plots. As can be seen, the bounds are much better for density (1); the values $Q_2(Z) \lesssim 1$ are consistent with all worldlines intersecting rather far from the laser-plasma interaction spacetime region. On the other hand, the large value of $Q_2(Z)$ for density (2) is an indication that worldlines intersect within or not far from the laser–plasma interaction spacetime region. Our computations lead to $Q_0(l'/20) = 10.64$, $Q_0(l'/2) =$ with density (1) and $Q_0(l'/20) = 88.53$, $Q_0(l'/2) = 32.35$ with density (2).

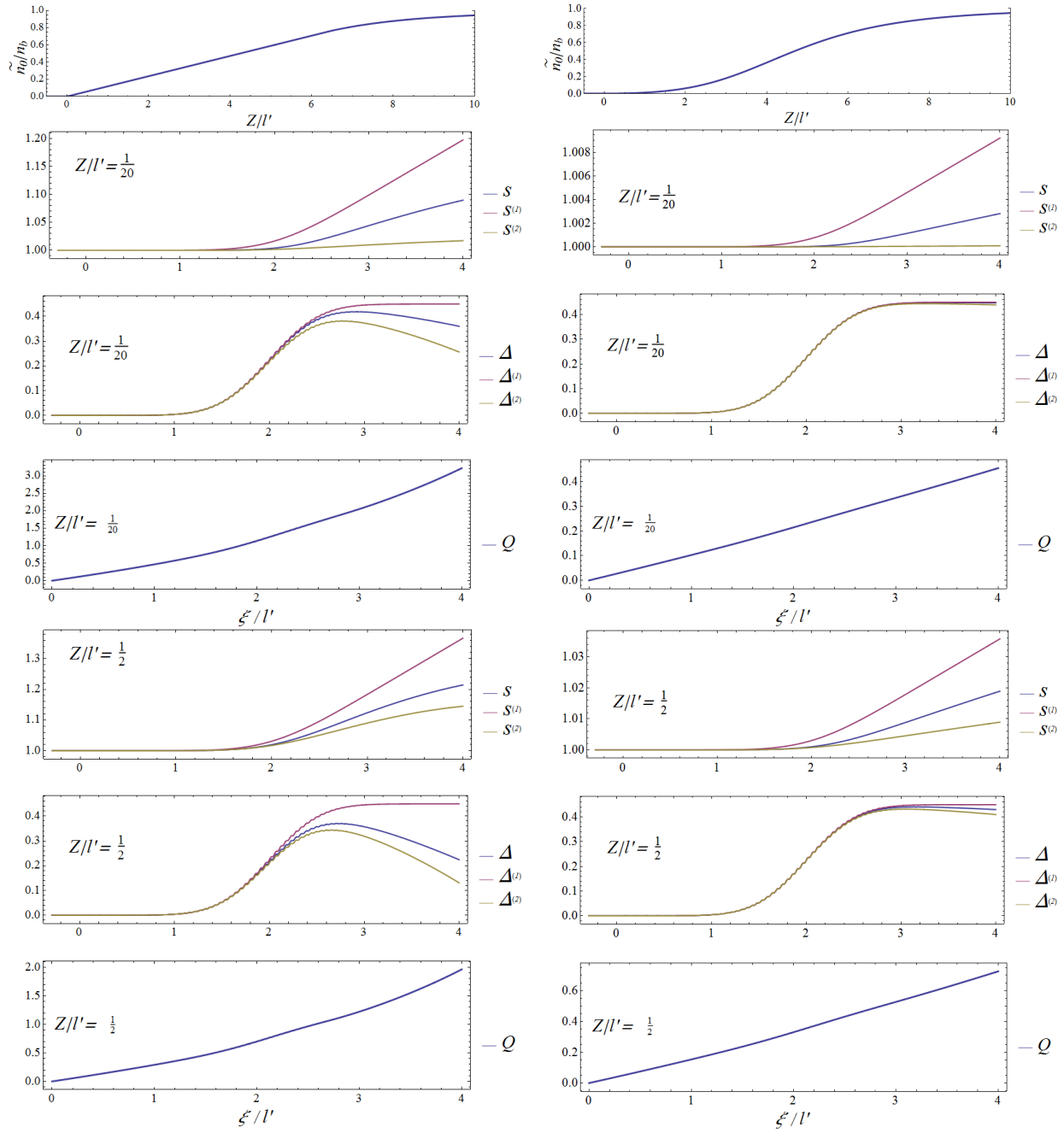

Figure 4. The initial electron densities (3), (4) of Figure 2 (left and right, respectively) with $n_b = 2 \times 10^{18}$ cm^{-3}, corresponding plots of s, Δ, their upper and lower bounds $s^{(1)}, s^{(2)}, \Delta^{(1)}, \Delta^{(2)}$, and the function $Q(\xi, Z)$, vs. ξ for the same sample values $Z = l'/20$ and $Z = l'/2$ of Z. The values $Q_2(Z) := Q(l, Z)$ can be read off the plots. As can be seen, the bounds are much better for density (4); the values $Q_2(Z) \leq 1$ are consistent with all worldlines intersecting rather far from the laser-plasma interaction spacetime region. On the other hand, the large value of $Q_2(Z)$ for density (3) is an indication that worldlines intersect not far from the laser–plasma interaction spacetime region. Our computations lead to $Q_0(l'/20) = 4.62$, $Q_0(l'/2) = 3.08$ with density (3) and $Q_0(l'/20) = 0.49$, $Q_0(l'/2) = 0.85$ with density (4).

3. Bounds on the Jacobian for Small $\xi > 0$

Differentiating (8), we find that the dimensionless variables

$$\varepsilon(\xi, Z) := J(\xi, Z) - 1 = \frac{\partial s(\xi, Z)}{\partial Z}, \qquad \sigma(\xi, Z) := l \frac{\partial s(\xi, Z)}{\partial Z} \tag{41}$$

fulfill the Cauchy problem

$$\begin{aligned} &\varepsilon' = -\kappa\sigma, \qquad \sigma' = Kl(\check{n} - \widetilde{n_0} + \check{n}\,\varepsilon), \\ &\varepsilon(0,Z) = 0, \quad \sigma(0,Z) = 0, \end{aligned} \tag{42}$$

where we have abbreviated $\kappa := \frac{1+v}{ls^3} \geq 0$. From σ, we can immediately obtain $\partial u^z/\partial Z$ via

$$l\frac{\partial u^z}{\partial Z} = -\frac{1+v}{2s^2}\,\sigma, \tag{43}$$

which is dimensionless, as well. To bound ε, σ for small ξ, we introduce the Liapunov function

$$V := \varepsilon^2 + \beta\sigma^2, \tag{44}$$

where $\beta(Z) \in \mathbb{R}^+$ is specified below. Clearly, $V(0,Z) = 0$. Equation (42) implies

$$V' \;\; = \;\; \varepsilon\sigma\, 2(\beta Kl\check{n} - \kappa) + \sigma\, 2\beta Kl(\check{n} - \widetilde{n_0}) \tag{45}$$

and as $2|\varepsilon\sigma| \leq V/\sqrt{\beta}$, $|\sigma| \leq \sqrt{V/\beta}$, we obtain

$$V' \leq 2A\sqrt{V} + 2BV \quad \Rightarrow \quad \left(\sqrt{V}\right)' \leq A + B\sqrt{V},$$

where we have abbreviated $B(\xi,Z) := |\beta Kl\check{n} - \kappa|/2\sqrt{\beta}$ and introduced some $A(Z)$ such that $A \geq Kl\sqrt{\beta}\max\{|\check{n} - \widetilde{n_0}|\}$. Per the comparison principle [38], $\sqrt{V} \leq R$, where $R(\xi,Z)$ is the solution of the Cauchy problem $R' = A + BR$, $R(0,Z) = 0$, which implies

$$|\varepsilon(\xi,Z)| \leq \sqrt{V(\xi,Z)} \leq R(\xi,Z) = A(Z)\int_0^\xi d\eta\, \exp\left[\int_\eta^\xi d\zeta\, B(\zeta,Z)\right] \tag{46}$$

and $\sqrt{b}|\sigma| \leq R$. As $R(\xi,Z)$ grows with ξ, if $R(l,Z) < 1$ then no WBDLPI may involve the Z-electrons. Choosing $\beta = 1/M_u l^2$, we find for all $\xi \in [0, \tilde{\xi}_3']$

$$2lB\,\beta = \left|\frac{1+v}{s^3} - \frac{\check{n}}{n_u}\right| \leq \left|\frac{1+v}{s^3} - 1\right| + \left|1 - \frac{\check{n}}{n_u}\right| \leq |D| + \delta,$$

$$\text{where} \qquad D(\xi,Z) := \frac{1+v(\xi)}{[s(\xi,Z)]^3} - 1, \quad \delta(Z) := 1 - \frac{n_d(Z)}{n_u(Z)}. \tag{47}$$

In the NR regime, which is characterized by $v \ll 1$, we have $s \simeq 1$, $\kappa \simeq 1/l$, $\Delta_u/l \ll 1$, $D \simeq 0$; setting $D = 0$ leads by a straightforward computation to

$$R(l,Z) \simeq R_{nr}(Z) := f[r(Z)], \qquad f(r) := 2\left(e^{r/2} - 1\right) \qquad r(Z) := \delta(Z)\sqrt{M_u(Z)}\,l.$$

As $f(r)$ grows with $r \geq 0$ and reaches the value 1 for $r \simeq 0.81$, we therefore find that the condition

$$r(Z) = \delta(Z)\sqrt{M_u(Z)}\,l < 0.81 \tag{48}$$

is sufficient to ensure that the Z-electrons are not involved in WBDLPI. This is automatically satisfied if $\sqrt{M_u(Z)}\,l < 0.81$, because by definition $\delta \leq 1$; otherwise, it is a very mild condition on the relative variation δ of the initial electron density across an interval of length $\Delta_u \ll l$ and in fact to violate (48) one needs a discontinuous (or a continuous and very steep) $\widetilde{n_0}(Z)$ with large relative variations around Z; see Section 4.

We now consider the general case. In the interval $[0,\tilde{\xi}_3']$, the inequalities $s^{(1)} \geq s \geq s^{(2)} \geq 1$ imply

$$\begin{aligned} |D(\xi,Z)| &\leq \mathcal{D}(\xi,Z) := \max\left\{ \frac{1+v(\xi)}{[s^{(2)}(\xi,Z)]^3} - 1\,,\, 1 - \frac{1+v(\xi)}{[s^{(1)}(\xi,Z)]^3} \right\} \\ &\leq \tilde{v}(\xi) := \max\{v(\xi),1\} \\ &\leq \max\{v_M,1\} =: \tilde{v}_M, \end{aligned} \tag{49}$$

where $v_M, \tilde{v}_M$ are the maxima of $v, \tilde{v}$. Hence, we obtain the bounds

$$\begin{aligned} \int_\eta^\xi d\zeta\, B(\zeta) &\leq \frac{\sqrt{M_u}}{2}\left[(\xi-\eta)\,\delta + \int_\eta^\xi d\zeta\, \mathcal{D}(\zeta)\right] \\ &\leq \frac{\sqrt{M_u}}{2}\left[(\xi-\eta)\,\delta + \int_\eta^\xi d\zeta\, \tilde{v}(\zeta)\right] \\ &\leq \frac{\sqrt{M_u}}{2}(\tilde{v}_M+\delta)(\xi-\eta), \end{aligned}$$

which are replaced in (46) by choosing $A = \sqrt{M_u}\,\delta$, respectively implying

$$R(\xi,Z) \leq \delta(Z)\sqrt{M_u(Z)}\int_0^\xi d\eta\, \exp\left\{\frac{\sqrt{M_u(Z)}}{2}\left[(\xi-\eta)\,\delta(Z) + \int_\eta^\xi d\zeta\, \mathcal{D}(\zeta,Z)\right]\right\} =: Q(\xi,Z) \tag{50}$$

$$Q(l,Z) \leq \delta(Z)\sqrt{M_u(Z)}\int_0^l d\eta\, \exp\left\{\frac{\sqrt{M_u(Z)}}{2}\left[(l-\eta)\,\delta(Z) + \int_\eta^l d\zeta\, \tilde{v}(\zeta)\right]\right\} =: Q_1(Z) \tag{51}$$

$$\leq \frac{2\delta(Z)}{\tilde{v}_M+\delta(Z)}\left\{\exp\left[\frac{\tilde{v}_M+\delta(Z)}{2}\sqrt{M_u(Z)}\,l\right] - 1\right\} =: Q_0(Z) \tag{52}$$

Here, we have redisplayed the Z-argument; $Q_2(Z) := Q(l,Z)$ is the most difficult to compute, while $Q_0(Z)$ is the easiest. We thus arrive at

Theorem 1. *Assume that condition (36) is fulfilled. Then, no WBDLPI involves the Z-electrons if in addition $Q_0(Z) < 1$, or at least $Q_1(Z) < 1$, or at least $Q_2(Z) < 1$. If one of these conditions is fulfilled for all Z, then WBDLPI occurs nowhere.*

Consequently, for any fixed pump there is no WBDLPI if n_b is sufficiently small. A simple sufficient condition is provided by the following corollary.

Corollary 1. *For any pulse (5) there is no WBDLPI if $Kn_b l^2 < 4\big[\log 2/(1+\tilde{v}_M)\big]^2$ and (36) are fulfilled. In particular, it suffices that $Kn_b l^2 < \min\big\{4\big[\log 2/(1+\tilde{v}_M)\big]^2, 2/(1+2\Delta_u/l)\big\}$.*

Proof. From $\delta \leq 1 \leq \tilde{v}_M$, it follows that $\delta\, l\, \sqrt{M_u} \leq L := \frac{\tilde{v}_M+\delta}{2}\, l\, \sqrt{M_b}$. Hence, $L < \log 2$ implies $e^L < 2$, whence

$$Q_0 = \delta\, l\, \sqrt{M_u}\, \frac{e^L-1}{L} \leq e^L - 1 < 1,$$

which, together with (36), implies the first claim. The second follows as well, as (40) implies (36). □

4. Discussion and Conclusions

As we have seen, if inequality (35) is fulfilled, then $\tilde{\xi}_2 > l$, i.e., the pulse is strictly short (that is, it completely overcomes the Z-electrons while their longitudinal displacement remains nonnegative). If at least inequality (36) is fulfilled, then $\tilde{\xi}_3 > l$, andt the pulse

is essentially short (that is, the pulse completely overcomes the Z-electrons before their longitudinal displacement reaches its first negative minimum), and the inequalities (27), (29), (50) and (52) apply. If in addition one of the conditions of Proposition 1 is satisfied, then WBDLPI can be excluded.

As seen above, the more easily computable (although more difficult to satisfy) condition (40) implies (35) and the inequality $M_u(Z)\,l^2 \le \frac{2}{1+2\Delta_u/l}$, which after substitution in (50) and (52) simplifies the computation of their rhs; in particular, (52) becomes

$$Q_0(Z) \le \frac{2\delta(Z)}{\tilde v_M+\delta(Z)}\left(e^C-1\right) =: \tilde Q_0(Z), \qquad C := \frac{\tilde v_M+\delta(Z)}{\sqrt{2[1+2\Delta_u/l]}}. \tag{53}$$

Therefore, (40) and $\tilde Q_0(Z) < 1$ provide a sufficient condition to exclude WBDLPI as well.

Note that in the above conditions, several dimensionless numbers characterizing the input data, viz. $\tilde v_M$, Δ_u/l, $G_b^2 = M_b l^2$, $M_u l^2$, $M_d l^2$, δ, and possibly s_u, $M_u' l^2$, play a key role in the main inequalities of the present paper. Therefore, their computation represents the first step in checking whether and where such conditions are fulfilled or violated.

In the NR regime (48) is equivalent to either inequality

$$\frac{n_d}{p} > \frac{n_u}{p} - \sqrt{\frac{2n_u}{p}} \quad\Leftrightarrow\quad \frac{n_u}{p} < 1 + \frac{n_d}{p} + \sqrt{1+2\frac{n_d}{p}}, \qquad p := \frac{(0.81)^2}{2Kl^2}. \tag{54}$$

(In fact, inequality (48) amounts to $n_u - n_d < \sqrt{2p\,n_u}$, i.e., (54); taking the square one obtains the equivalent inequality $n_u^2 - 2n_u(n_d+p)+n_d^2 < 0$, which is fulfilled if $n_- < n_u < n_+$, where $n_\pm := n_d+p\pm\sqrt{(n_d+p)^2-n_d^2} = n_d+p\pm\sqrt{p^2+2pn_d}$ solve the equation $x^2-2x(n_d+p)+n_d^2 = 0$ in the unknown x; the left inequality is automatically satisfied because $n_u \ge n_d > n_d^2/n_+ = n_-$. Dividing the inequality $n_u < n_+$ by p, we obtain (54)).

If $\widetilde{n_0}$ grows in $[0, \bar Z+\Delta_u]$, then $q(z) := \widetilde{n_0}(z)/p$ does as well, and for all $\in [0,\bar Z]$ the previous conditions become

$$q(Z) > q\big(Z+\Delta_u\big) - \sqrt{2q\big(Z+\Delta_u\big)} \quad\Leftrightarrow\quad q\big(Z+\Delta_u\big) < 1+q(Z)+\sqrt{1+2q(Z)}. \tag{55}$$

This is fulfilled if, e.g., in $[0,\bar Z+\Delta_u]$ $\widetilde{n_0}$ is continuous (without excluding $\widetilde{n_0}(0^+) > 0$), at least piecewise C^1, and $0 \le \frac{dq(z)}{dz}\,\Delta_u < 1+\sqrt{1+2q(Z)}$ for all $Z \in [0,\bar Z]$ and $z \in [Z, Z+\Delta_u]$.

Now, we impose that $\widetilde{n_0}$ is continuous in $[-\infty, \bar Z+\Delta_u]$ and reaches a given value $\bar n > 0$ at $Z = \bar Z$ while respecting (55). We compare the minimum $\bar Z$ for a linear and a quadratic $\widetilde{n_0}$; note that dq/dZ for the former violates the above bound at $Z = 0$. We find

$$\widetilde{n_0}(Z) = n_1(Z) := \theta(Z)\bar n\frac{Z}{\bar Z} \quad \text{fulfills (55) if} \quad \frac{\bar Z}{\Delta_u} > \frac{\bar n}{2p} = \frac{K\bar n l^2}{(0.81)^2} =: \frac{\bar Z_1}{\Delta_u} \tag{56}$$

$$\widetilde{n_0}(Z) = n_2(Z) := \theta(Z)\bar n\frac{Z^2}{\bar Z^2} \quad \text{fulfills (55) if} \quad \frac{\bar Z}{\Delta_u} > \sqrt{\frac{\bar n}{2p}}+\sqrt{\frac{\bar n}{2p}+\frac14}-\frac12 =: \frac{\bar Z_2}{\Delta_u} \tag{57}$$

where θ is the Heavisde step function. In fact, if $\widetilde{n_0} = n_1$, then (55 Right) becomes $\bar n\Delta_u/p\bar Z < 1+\sqrt{1+2\bar n Z/p\bar Z}$ for all Z; the rhs is lowest for $Z = 0$, whereby the inequality becomes (56 Right), as claimed. If $\widetilde{n_0} = n_2$, then (55 Left) becomes the condition

$$F(Z) := \sqrt{\frac{2p}{\bar n}}\bar Z(Z+\Delta_u) - \Delta_u^2 - 2\Delta_u Z > 0;$$

this is of first degree in Z, and is hence fulfilled for all $Z \in [0,\bar Z]$ if it is for $Z = 0, \bar Z$. The quadratic polynomial $F(\bar Z)$ in $\bar Z$ is positive if $\bar Z > Z_2$, as claimed, because Z_2 is the positive

solution of the equation $F(z) = 0$ in the unknown z, and $\bar{Z} > Z_2$ automatically makes $F(0) > 0$.

If $\sqrt{K\bar{n}}\,l$ is considerably larger than 1, then $\bar{Z}_1$ is considerably larger than $\bar{Z}_2$; in particular, assuming (2) with $n_b = \bar{n}$, i.e., $G_b \sim \pi$, yields $Z_1 \sim 15.04\Delta_u$, $Z_2 \sim 6.78\Delta_u$. Therefore, choosing $\bar{Z} \in]Z_2, Z_1[$, we can exclude WBDLPI by adopting $\widetilde{n_0}(Z) = n_2(Z)$, but not $\widetilde{n_0}(Z) = n_1(Z)$. Such a result is relevant for LWFA experiments, which usually fulfill (2). From the physical viewpoint, it allows us to exclude WBDLPI because: (i) the density $\widetilde{n_0}(Z)$ obtained just outside the nozzle of a supersonic gas jet (orthogonal to the $\vec{z}$) typically is $C^1(\mathbb{R})$, with $\widetilde{n_0}(0) = 0 = \frac{d\widetilde{n_0}}{dZ}(0)$ (see, e.g., Figure 2 in [39] or Figure 5 in [40]), and therefore is closer to type $n_2(Z)$ than to type $n_1(Z)$; and (ii) by causality, the effects of a pulse with a finite spot radius R near its symmetry axis $\vec{z}$ are the same as with a plane wave ($R = \infty$), at least for small ξ. From the viewpoint of mathematical modeling, this suggests that it makes a major difference whether we describe the edge of the plasma by n_1 or by n_2; in the first case, we can correctly predict the plasma evolution only by kinetic theory and PIC codes, while in the second we can do this by a hydrodynamic description and less computationally demanding multifluid codes.

If we allow a discontinuous (in $Z = 0$) linear Ansatz $\widetilde{n_0}(Z) = \theta(Z)\bar{n}[a + (1-a)Z/\bar{Z}]$ ($0 < a \leq 1$), then (55) is fulfilled if $\bar{Z} > \bar{n}(1-a)\Delta_u / p[1+\sqrt{1+2a\bar{n}/p}]$, which is again smaller than Z_1.

Although our results apply to all $\boldsymbol{\epsilon}^\perp$ with support contained in $[0, l]$, regardless of their Fourier analysis, in most applications one deals with a modulated monochromatic wave

$$\boldsymbol{\epsilon}^\perp(\xi) = \underbrace{\epsilon(\xi)}_{\text{modulation}} \underbrace{[\mathbf{i}\cos\psi\,\sin(k\xi+\varphi_1)+\mathbf{j}\sin\psi\sin(k\xi+\varphi_2)]}_{\text{carrier wave } \boldsymbol{\epsilon}_o^\perp(\xi)}, \tag{58}$$

where $\mathbf{i} = \nabla x$, $\mathbf{j} = \nabla y$. The elliptic polarization in (58) is ruled by $\psi, \varphi_1, \varphi_2$; it reduces to a linear one in the direction of $\boldsymbol{a} := \mathbf{i}\cos\psi + \mathbf{j}\sin\psi$ if $\varphi_1 = \varphi_2$, to a circular one if $|\cos\psi| = |\sin\psi| = 1/\sqrt{2}$ and $\varphi_1 = \varphi_2 \pm \pi/2$. If, as follows from (1), $Kn_b\lambda^2 \ll 1$ ($\lambda = 2\pi/k$ is the wavelength), i.e., the plasma is underdense, then the relative variations of $\Delta(\xi, Z)$ (and $z_e(\xi, Z)$) in a ξ-interval of length $\leq \lambda$ are much smaller than those of $\boldsymbol{x}_e^\perp(\xi)$, and those of $s(\xi)$ even smaller; in fact, as $s > 0$, $v \geq 0$, the integral in (13 Left) averages the fast variations of v to yield much smaller relative variations of Δ, and the first integral in (13 Right) averages the residual small variations of $\widetilde{N}[z_e(\xi)]$ to yield an essentially smooth $s(\xi)$ (see, e.g., Figure 1). On the contrary, $\boldsymbol{\alpha}^\perp(\xi), \boldsymbol{x}_e^\perp(\xi)$ varies fast, as $\boldsymbol{\epsilon}^\perp(\xi)$. Under rather general assumptions (see Appendix 5.2) [31],

$$\boldsymbol{\alpha}^\perp(\xi) = -\frac{\epsilon(\xi)}{k}\,\boldsymbol{\epsilon}_p^\perp(\xi) + O\left(\frac{1}{k^2}\right) \simeq -\frac{\epsilon(\xi)}{k}\,\boldsymbol{\epsilon}_p^\perp(\xi), \tag{59}$$

where $\boldsymbol{\epsilon}_p^\perp(\xi) := \boldsymbol{\epsilon}_o^\perp(\xi + \lambda/4)$, and similarly for other integrals with modulated integrands. In the appendix, we recall upper bounds for the remainders $O(1/k^2)$. If $|\epsilon'| \ll |k\epsilon|$ (slow modulations); the right estimate is very good, and v can be approximated very well by $v \simeq \boldsymbol{\epsilon}_p^{\perp 2}\left(e\epsilon/kmc^2\right)^2$. For the reasons mentioned above, replacing v by its (approximated) average over a cycle,

$$v_a(\xi) := \frac{1}{2}\left(\frac{e\,\epsilon(\xi)}{kmc^2}\right)^2, \tag{60}$$

has only a small effect on Δ and almost no effect on s, V, and similarly on the functions $\Delta^{(0)}, s^{(1)}, \ldots$ introduced in Sections 2 and 3 to bound Δ, s, V; however, it simplifies their computation a great deal. As a consequence, the bounds (27), (29) and (37), as well as the short pulse conditions (35) and (36) and the no-WB conditions of proposition 1, remain essentially valid if in computing the bounds we replace v with v_a.

We illustrate the results obtained thus far considering a pulse (58) with a linear polarization (e.g., $\psi = 0$) and a modulation of Gaussian type, except that it is cut off outside of support $0 \leq \xi \leq l$:

$$\frac{e}{kmc^2}\,\epsilon(\xi) = a_0\,\exp\left[-\frac{(\xi - l/2)^2}{l'^2}2\log 2\right]\theta(\xi)\,\theta(l-\xi); \tag{61}$$

where l' is the *full width at half maximum* of the intensity I of the electromagnetic (EM) field. More precisely, we adopt the pulse plotted in Figure 1a, which has its maximum at $\xi = l/2$ and $a_0 = 1.3$; this yields a moderately relativistic electron dynamics and $\Delta_u \equiv \Delta^{(0)}(l) \simeq 0.45l'$. In Figure 1b, we plot the associated v and v_a. We performed all computations and plots running our specifically designed programs using an "off the shelf" general-purpose numerical package on a common notebook for an elapsed time bewteen several seconds and several minutes. Here, we compare the impact of such a pulse on the density profiles plotted in Figure 2.

The upper bound n_b plays the role of asymptotic value. Here, we choose $n_b = 2 \times 10^{18}\ \mathrm{cm}^{-3}$, which is the same as the n_0 of Figure 1, which yields $Kn_b l'^2 \simeq 4$; however, the results for the dimensionless variables remain the same if we change n_b, λ, l' while keeping λ/l' and $Kn_b l'^2$ constant. As already stated, in the case of the step-shaped density 0), if $\tilde{\xi}_2 > l$, i.e., if the pulse is strictly short (a sufficient condition for which is (35)), then $n_u = n_d = n_b$, $\delta = 0$, and by (50) and (52) there is no WBDLPI; more directly, this is a consequence of $J(\xi, Z) \equiv 1$ for $0 \leq \xi \leq l$, which follows from the Z-independence of Δ in such an interval. As for the other profiles, we have respectively plotted the following:

- In Figures 5 and 6, the solutions J, σ of Equation (42) and, by (43), the associated function $l'\partial u^z/\partial Z$ for $0 \leq \xi \leq 6l'$ and a few values of Z, assuming the initial electron density profiles (1), (2) and (3), and (4), respectively.
- In Figures 3 and 4, the solutions s, Δ of (8) and (9), their upper and lower bounds $s^{(1)}, s^{(2)}, \Delta^{(1)}, \Delta^{(2)}$ (Equation (28)), and the function Q of Equation (50) for $0 \leq \xi \leq 6l'$ and a few values of Z, assuming the initial electron density profiles (1)–(4), respectively.
- In Figures 7 and 8, the corresponding worldlines of the Z-electrons for $0 \leq ct \leq 20l'$ and $Z = n\,l'/20$, $n = 0, 1, ..., 200$ associated with the initial electron density profiles (3) and (4). The support of the EM pulse is coloured pink (the red part is the more intense part); the laser–plasma interaction takes place in the spacetime region which has nonempty intersection with worldlines of electrons or protons.

We compare the results for densities (1)–(2) and those for densities (3)–(4) side by side. In case (1), WBDLPI is avoided assuming that $\widetilde{n_0}(0) > 0$, although worldlines intersect and WB takes place not far from the laser–plasma interaction region. In case (2), WBDLPI takes place for $Z \simeq 0$ due to the steep growth of $\widetilde{n_0}(Z) = Z/l'n_b$ from the value $\widetilde{n_0}(0) = 0$. In case (3), although the growth $\widetilde{n_0}(Z) \propto Z$ is much less steep, again worldlines intersect and WB takes place not very far from the laser–plasma interaction region. Finally, in case (4) this occurs quite far from the latter, consistently with the results $|J - 1| \ll 1$, $Q_2 < 1$. Thus, we note that although such dynamics are moderately relativistic rather than nonrelativistic, switching from profile (1) to profile (2) or from profile (3) to profile (4) has the same qualitative effect of avoiding (or distancing from) WBDLPI. We additionally note that in cases (1) and (3) the $Z \simeq 0$ worldlines first intersect with very small angles, or equivalently that when the corresponding electrons collide their longitudinal momenta differ by only a very small amount. By Formula (43), $l\partial u^z/\partial Z$ is very small both because σ is as well and because $v \simeq 0$ and $s > 1$. Hence, we can expect that these collisions will lead only to very small momentum spreading.

Essentially the same results are reached when choosing a different pulse polarization, because v_a is of the same type. In the case of circular polarization ($\varphi_1 - \varphi_2 = \pm\pi/2$, $\cos\psi = \pm\sin\psi$) and Gaussian modulation v, it will itself essentially coincide with v_a, thus displaying a single maximum (see Figure 1b).

As mentioned in the introduction, the equations of motion for the Z-electrons can be reduced to the form (8), and thus are *decoupled* from those of all Z'-electrons, $Z' \neq Z$, only in the idealization where the laser pulse is "undepleted", i.e., not affected by its interaction with the plasma. The latter is expected to be an acceptable approximation only for small $t, z > 0$. Actually, for a slowly modulated monochromatic wave we can show by self-consistency [28] that this is a good approximation in the spacetime region that is the intersection of the 'laser–plasma interaction' stripe $0 \leq ct - z \leq l$ with the orthogonal stripe

$$0 \leq \frac{e^2 n_b \lambda}{2mc^2}(ct + z) \ll 1. \tag{62}$$

In view of the inequalities $\lambda \ll l$ and (1) or (16), we can see that, to our satisfaction, this region is much longer than l in the $ct+z$ direction. Thus, if $n_b = 2 \times 10^{18}\text{cm}^{-3}$ and the pulse is as in Figure 1, we can consider the latter as undepleted and the electrons' motion determined above as accurate for time intervals $[0, t_d]$, where t_d is at least a few 10^{-13}s.

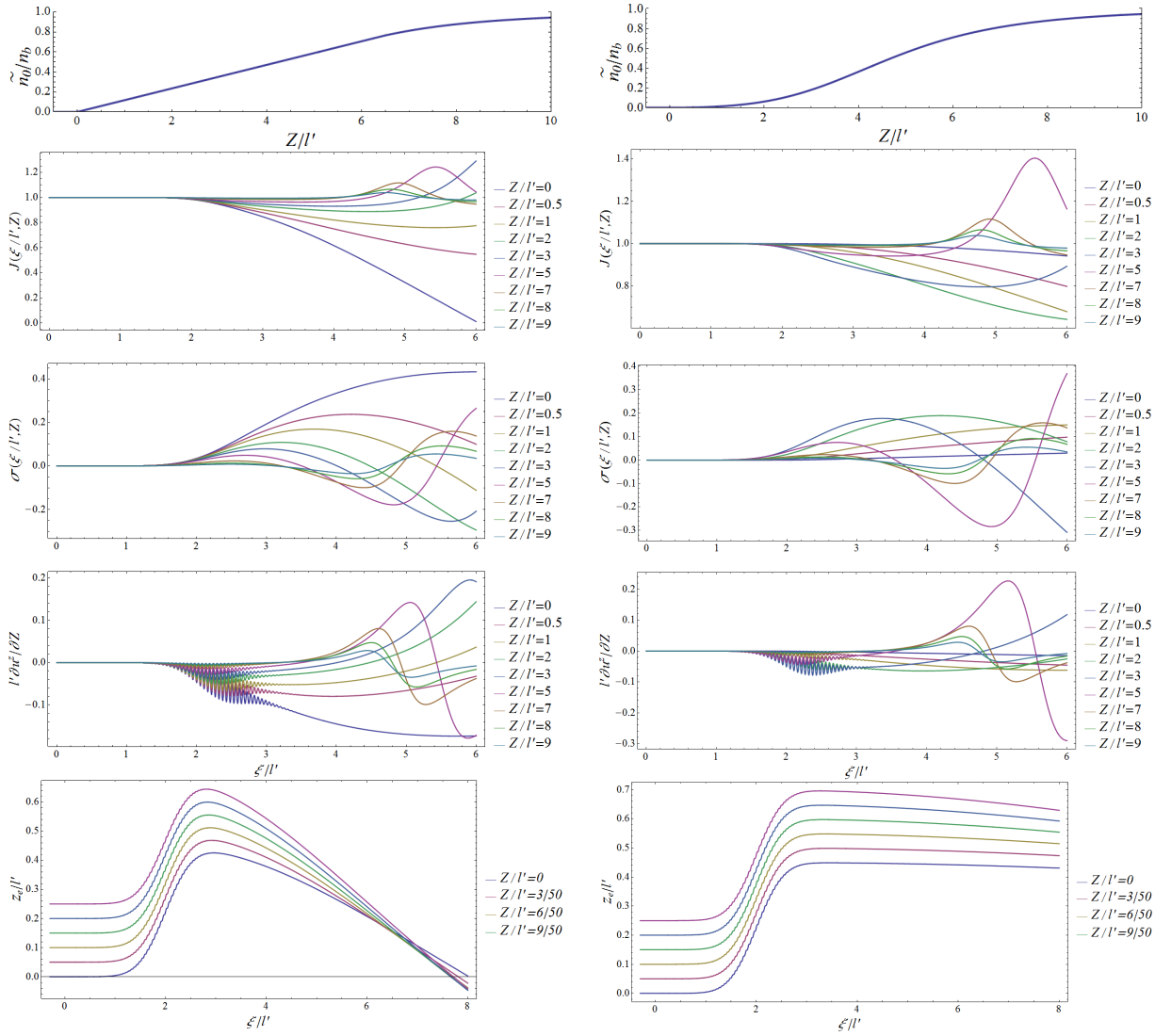

Figure 5. The initial electron densities (3), (4) of Figure 2 (left and right, respectively) with $n_b = 2 \times 10^{18}$ cm^{-3}, and below, the corresponding plots of $J, \sigma, l'\partial u^z/\partial z$ during interaction with the pulse in Figure 1 for a few sample values of Z. As can be seen, J remains positive at least for all $\xi \in [0, 2l]$ if the density is of type (4) (which grows as Z^2 for $Z \sim 0$), whereas it becomes negative for $\xi \sim 6.5l'$ and small Z if the density is of type (3) (which grows as Z for $Z \sim 0$). Correspondingly, the right-hand worldlines do not intersect, while the left-hand ones do (see the down z_e-graphs).

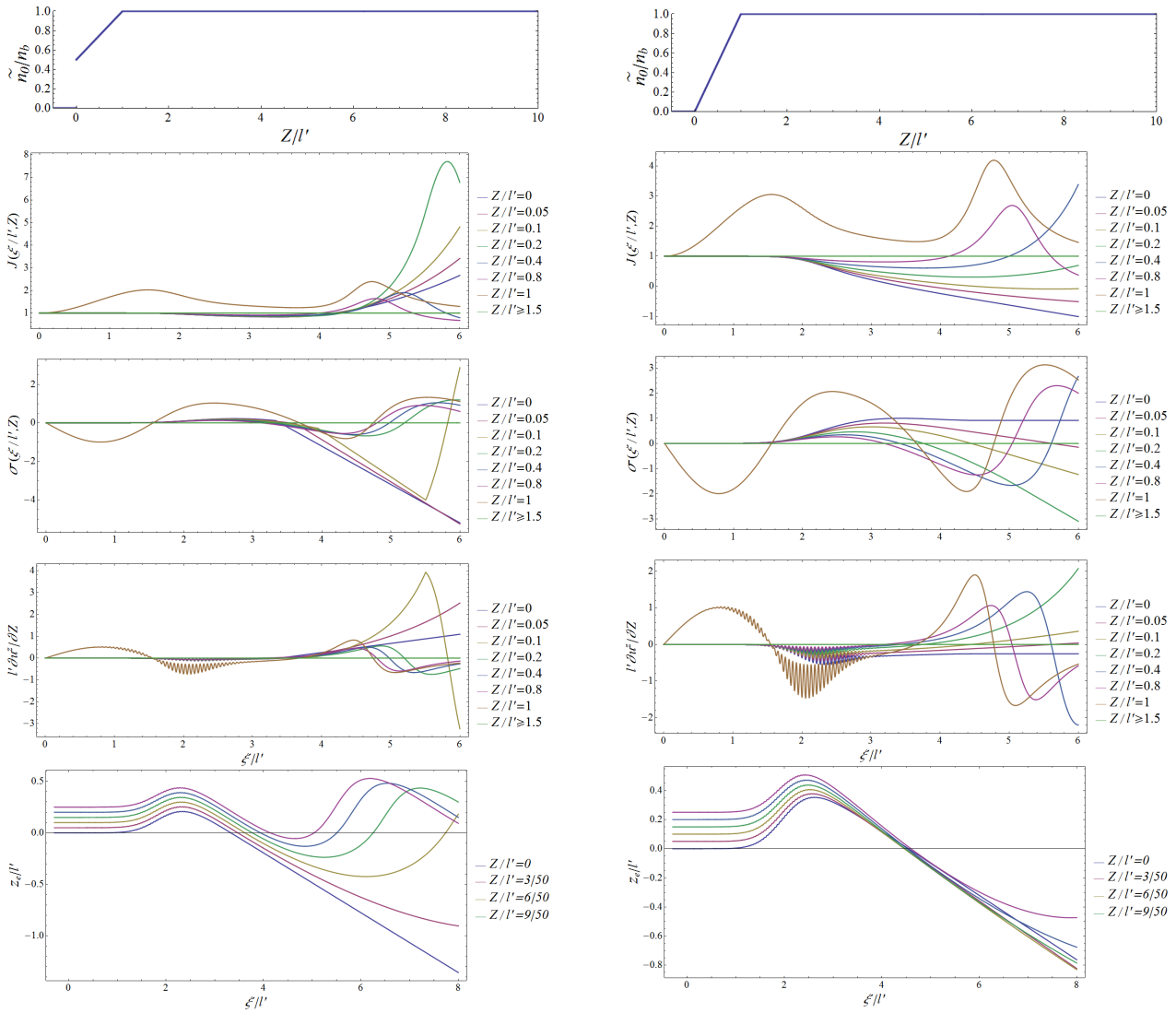

Figure 6. The initial electron densities (1), (2) of Figure 2 (first line; respectively left, right), and below, the corresponding plots of $J, \sigma, l'\partial u^z/\partial z$ vs. ξ during interaction with the pulse in Figure 1 for a few sample values of Z. As can be seen, the right J remains positive for $\xi < l$ and all Z, while the left J becomes negative for very small Z and $\xi \lesssim l$; correspondingly, the right worldlines do not intersect, while the right ones do (see the down z_e-graphs).

The above predictions are based on idealizing the initial laser pulse as a plane EM wave (5). In a more realistic picture, the $t = 0$ laser pulse is cylindrically symmetric around the $\vec{z}$-axis and has a *finite* spot radius R, namely, the $t = 0$ EM fields are of the form $\boldsymbol{E} = \boldsymbol{\epsilon}^{\perp}(-z)\,\chi(\rho)$, $\boldsymbol{B} = \mathbf{k}\times\boldsymbol{E}$, where $\rho^2 = x^2+y^2$, while $\chi(\rho) \geq 0$ is 1 for $\rho \leq 1$ and rapidly approaches zero for $\rho > R$. By causality, the motion of the electrons remains [25] strictly the same in the future Cauchy development $D^+(\mathcal{D})$ of $\mathcal{D} = \mathcal{D}_1 \cup \mathcal{D}_2$, where $\mathcal{D}_1 := \{(ct,\boldsymbol{x}) = (0,0,0,z > 0\}$ and $\mathcal{D}_2 := \{(0,\boldsymbol{x}) \,|\, \rho \leq R\}$, and almost the same in a neighbourhood of $D^+(\mathcal{D})$; therefore, the conditions described above remain sufficient to exclude WBDLPI at least in such a region. (Recall that the *future Cauchy development* $D^+(\mathcal{D})$ of a region $\mathcal{D}$ in Minkowski spacetime M^4 is defined as the set of all points $x \in M^4$ for which every past-directed causal, i.e., non-spacelike, line through x intersects $\mathcal{D}$.)

Finally, the conditions of Proposition 1 are very general in that they apply to discontinuous $\widetilde{n_0}$ or non-monotone $\widetilde{n_0}$; however, if $\widetilde{n_0}$ has a bounded derivative, it turns out that they are unnecessarily too strong for ensuring that no WBDLPI occurs. Weaker no-WBDLPI conditions under the latter assumptions are treated in [28].

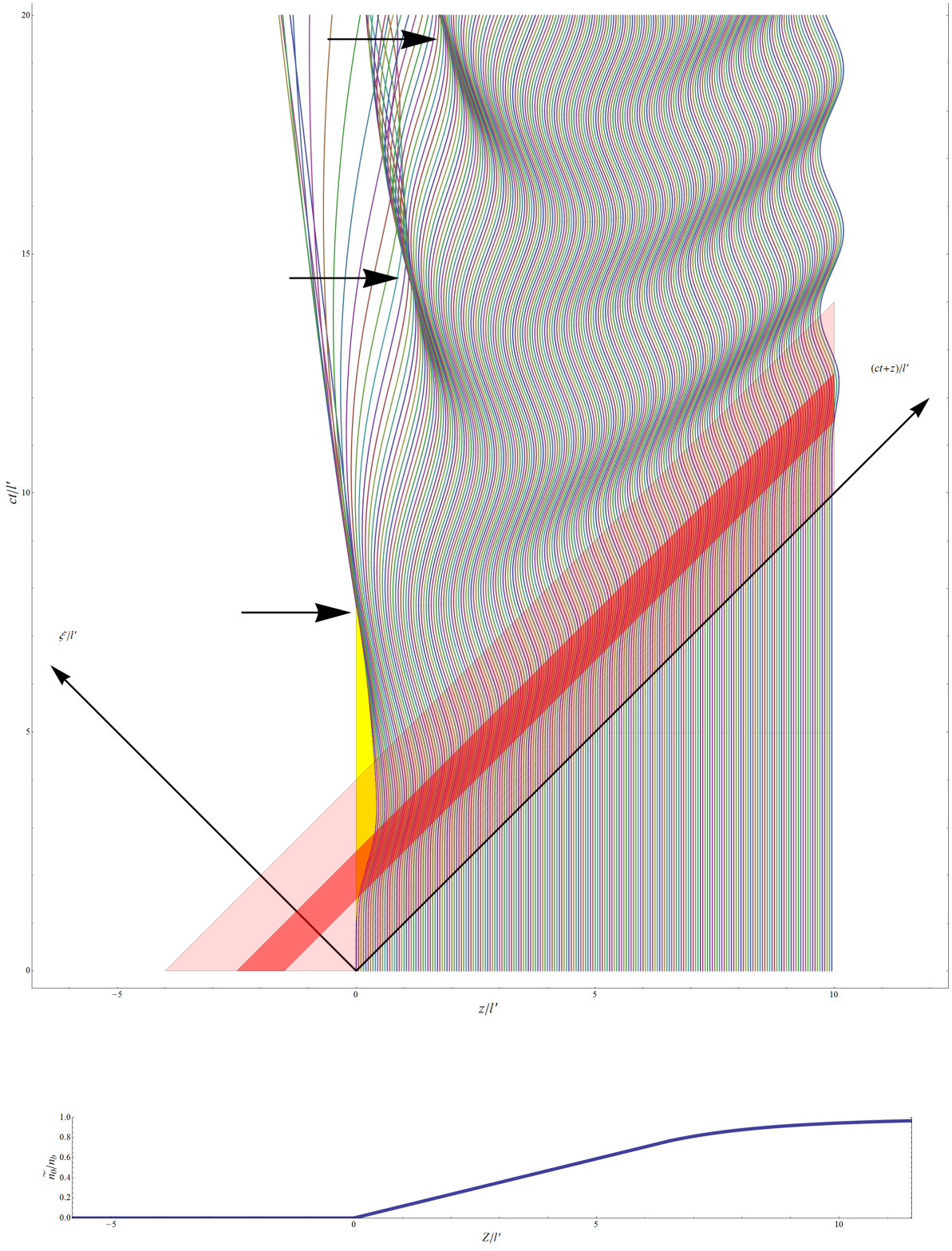

Figure 7. Down: the initial electron density (3) of Figure 2. **Up**: The worldlines of Z-electrons interacting with the pulse in Figure 1 for 200 equidistant values of Z; the support $0 \leq ct-z \leq l$ and the 'effective support' $(l-l')/2 \leq ct-z \leq (l+l')/2$ of the pulse are pink and red;, respectively, while the spacetime region of the pure-ion layer is yellow. Horizontal arrows pinpoint where particular subsets of worldlines first intersect.

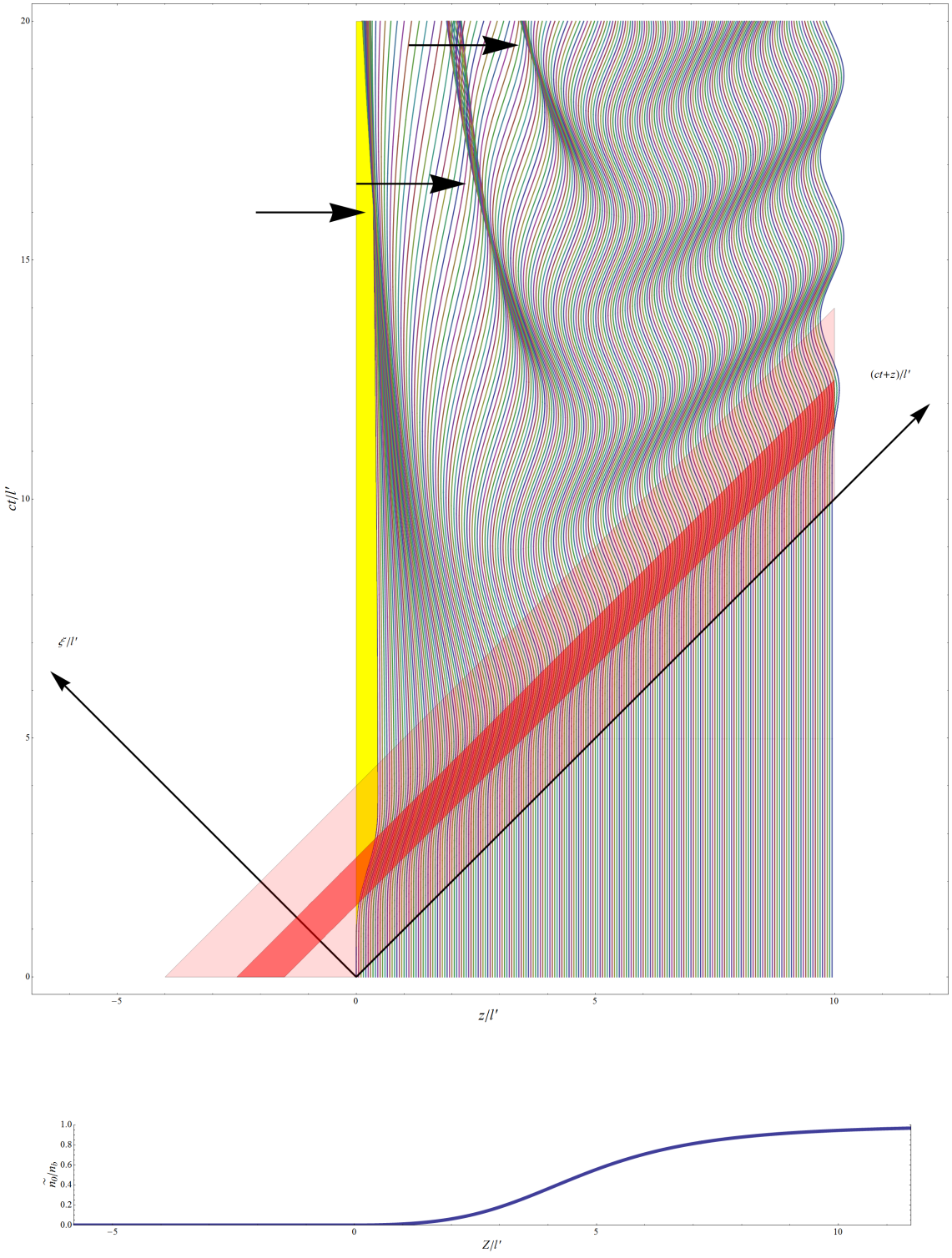

Figure 8. Down: The initial electron density (4) of Figure 2. **Up**: The worldlines of Z-electrons interacting with the pulse in Figure 1 for 200 equidistant values of Z; the support $0 \leq ct-z \leq l$ and the 'effective support' $(l-l')/2 \leq ct-z \leq (l+l')/2$ of the pulse are pink and red, respectively, while the spacetime region of the pure-ion layer is yellow. Horizontal arrows pinpoint where particular subsets of worldlines first intersect; as can be seen, small Z worldlines first intersect quite farther from the laser–plasma interaction spacetime region (shown in pink) than in the linear homogenous case (3).

Author Contributions: Conceptualization, G.F., R.F. and D.J.; Formal analysis, G.F.; Investigation, G.F.; Methodology, M.D.A. and G.G.; Validation, D.J.; Visualization, G.F.; Writing, original draft, G.F.; Writing, review and editing, M.D.A., R.F., G.G. and D.J. All authors have read and agreed to the published version of the manuscript.

Funding: This research received no external funding.

Institutional Review Board Statement: Not applicable.

Informed Consent Statement: Not applicable.

Data Availability Statement: Not applicable.

Conflicts of Interest: The authors declare no conflict of interest.

Appendix A

Appendix A.1. Proof of Proposition 1

We abbreviate $\Omega := \sqrt{Kn_b}$, $\zeta := l - \eta$. Equation (17) yields

$$\begin{aligned}
2\Delta(l) &= \int_0^{l/2} d\eta\, v(\eta)\, \cos[\Omega(l-\eta)] + \int_{l/2}^{l} d\eta\, v(l-\eta)\, \cos[\Omega(l-\eta)] \\
&= \int_0^{l/2} d\eta\, v(\eta)\, \cos[\Omega(l-\eta)] - \int_{l/2}^{0} d\zeta\, v(\zeta)\, \cos(\Omega\zeta) \\
&= \int_0^{l/2} d\eta\, v(\eta)\, \cos[\Omega(l-\eta)] + \int_0^{l/2} d\eta\, v(\eta)\, \cos(\Omega\eta) \\
&= [1+\cos(\Omega l)] \int_0^{l/2} d\eta\, v(\eta) \cos(\Omega\eta) + \sin(\Omega l) \int_0^{l/2} d\eta\, v(\eta) \sin(\Omega\eta) \qquad \text{(A1)} \\
2\delta(l) &= \int_0^{l/2} d\eta\, v(\eta)\, \sin[\Omega(l-\eta)] + \int_{l/2}^{l} d\eta\, v(l-\eta)\, \sin[\Omega(l-\eta)] \\
&= \int_0^{l/2} d\eta\, v(\eta)\, \sin[\Omega(l-\eta)] - \int_{l/2}^{0} d\zeta\, v(\zeta)\, \sin(\Omega\zeta) \\
&= [1-\cos(\Omega l)] \int_0^{l/2} d\eta\, v(\eta) \sin(\Omega\eta) + \sin(\Omega l) \int_0^{l/2} d\eta\, v(\eta) \cos(\Omega\eta) \qquad \text{(A2)}
\end{aligned}$$

If $\Omega l \leq \pi$, both integrands in (A1) are nonnegative, as are the factors of both integrals, and moreover the latter and $\Delta(l)$ itself are positive if $\Omega l < \pi$ and zero if $\Omega l = \pi$. In either case, $\Delta(\xi) > 0$ for all $\xi \in]0, l[$, because $\Delta'(l) = v(l) - \delta(l) < 0$ (as $v(l) \simeq 0$, $\delta(l) > 0$). Moreover, if $\varepsilon := \Omega l - \pi > 0$ is sufficiently small, then both integrals and $1+\cos(\Omega l) = 1-\cos\varepsilon \simeq \varepsilon^2/2$ are positive, whereas $\sin(\Omega l) = -\sin\varepsilon \simeq -\varepsilon$; the second negative term will dominate and make (A1) negative as well. Therefore, (17 Left) will be satisfied iff $\Omega l \leq \pi$, i.e., if $G_b \leq 1/2$.

Similarly, if $\Omega l = 2\pi$, the factors of both integrals in (A2) vanish, and $\delta l = 0$. If $\varepsilon := \Omega l - 2\pi \neq 0$ is sufficiently small, then $1-\cos(\Omega l) = 1-\cos\varepsilon \simeq \varepsilon^2/2$, whereas $\sin(\Omega l) = \sin\varepsilon \simeq \varepsilon$, and the second term dominates over the first. Under our assumptions, the second integral will be negative, because $v(\eta)$ is larger where $\cos(\Omega\eta) < 0$. Hence, (A2) will be negative if $\varepsilon > 0$ (and is sufficiently small); if $\varepsilon < 0$ (and is sufficiently small), then (A2) will be positive, and $\delta(\xi) > 0$ for $0 < \xi < l$, because $\delta'(l) = M\Delta(l) < 0$ (as in this case $\Delta(l) < 0$. Therefore, (17 Right) will be satisfied iff $\Omega l \leq 2\pi$, i.e., if $G_b \leq 1$.

Appendix A.2. Estimates of Oscillatory Integrals

Here, we recall useful estimates [31] of oscillatory integrals such as (6 Left) in case (58). Given a function $f \in C^2(\mathbb{R})$, integrating by parts we find that for all $n \in \mathbb{N}$

$$\int_{-\infty}^{\xi} d\zeta\, f(\zeta) e^{ik\zeta} = -\frac{i}{k} f(\xi) e^{ik\xi} + R_1^f(\xi), \tag{A3}$$

$$R_1^f(\xi) := \frac{i}{k}\int_{-\infty}^{\xi} d\zeta\, f'(\zeta)\, e^{ik\zeta} = \left(\frac{i}{k}\right)^2 \left[-f'(\xi)\, e^{ik\xi} + \int_{-\infty}^{\xi} d\zeta\, f''(\zeta)\, e^{ik\zeta}\right]. \tag{A4}$$

Hence, we find the following upper bounds for the remainder R_1^f:

$$\left|R_1^f(\xi)\right| \le \frac{1}{|k|^2}\left[|f'(\xi)| + \int_{-\infty}^{\xi} d\zeta\, |f''(\zeta)|\right] \le \frac{\|f'\|_\infty + \|f''\|_1}{|k|^2}, \tag{A5}$$

It follows that $R_1^f = O(1/k^2)$. All inequalities in (A5) are useful; the left inequalities are more stringent, while the right ones are ξ-independent.

Equations (A3) and (A5) and $R_1^f = O(1/k^2)$ hold if $f \in W^{2,1}(\mathbb{R})$ (a Sobolev space), and in particular if $f \in C^2(\mathbb{R})$ and $f, f', f'' \in L^1(\mathbb{R})$, because the previous steps can be performed under such assumptions. Equations (A3) will hold with a remainder $R_1^f = O(1/k^2)$ under weaker assumptions, e.g., if f' is bounded and piecewise continuous and $f, f', f'' \in L^1(\mathbb{R})$, although R_1^f will be a sum of contributions such as (A4) for every interval in which f' is continuous.

Letting $\xi \to \infty$ in (A3), (A5) we find for the Fourier transform $\tilde{f}(k) = \int_{-\infty}^{\infty} d\zeta\, f(\zeta) e^{-iky}$ of $f(\xi)$

$$|\tilde{f}(k)| \le \frac{\|f'\|_\infty + \|f''\|_1}{|k|^2}, \tag{A6}$$

hence, $\tilde{f}(k) = O(1/k^2)$ as well. Actually, if $f \in \mathcal{S}(\mathbb{R})$, then $\tilde{f}(k)$ decays much faster, as $|k| \to \infty$, because $\tilde{f} \in \mathcal{S}(\mathbb{R})$ as well. For instance, if $f(\xi) = \exp[-\xi^2/2\sigma]$, then $\tilde{f}(k) = \sqrt{\pi\sigma}\exp[-k^2\sigma/2]$.

To prove approximation (59), now we just need to choose $f = \epsilon$ and note that every component of $\boldsymbol{\alpha}^\perp$ will be a combination of (A3) and $(A3)_{k\mapsto -k}$.

References

1. Kruer, W. *The Physics Of Laser Plasma Interactions*; CRC Press: Boca Raton, FL, USA, 2019; 200p.
2. Sprangle, P.; Esarey, E.; Ting, A. Nonlinear interaction of intense laser pulses in plasmas. *Phys. Rev.* **1990**, *A41*, 4463. [CrossRef] [PubMed]
3. Sprangle, P.; Esarey, E.; Ting, A. Nonlinear Theory of Intense Laser-Plasma Interactions, *Phys. Rev. Lett.* **1990**, *64*, 2011. [CrossRef] [PubMed]
4. Esarey, E.; Schroeder, C.B.; Leemans, W.P. Physics of laser-driven plasma-based electron accelerators. *Rev. Mod. Phys.* **2009**, *81*, 1229. [CrossRef]
5. Macchi, A. *A Superintense Laser-Plasma Interaction Theory Primer*; Springer: Berlin/Heidelberg, Germany, 2013.
6. Kuzenov, V.V.; Ryzhkov, S.V. Numerical simulation of the effect of laser radiation on matter in an external magnetic field. *J. Phys. Conf. Ser.* **2017**, *830*, 012124.
7. Tajima, T.; Dawson, J.M. Laser Electron Accelerator. *Phys. Rev. Lett.* **1979**, *43*, 267. [CrossRef]
8. Sprangle, P.; Esarey, E.; Ting, A.; Joyce, G. Laser wakefield acceleration and relativistic optical guiding. *Appl. Phys. Lett.* **1988**, *53*, 2146. [CrossRef]
9. Tajima, T.; Nakajima, K.; Mourou, G. Laser acceleration. *Riv. N. Cim.* **2017**, *40*, 34. [CrossRef]
10. Hidding, B.; Beaton, A.; Boulton, L.; Corde, S.; Doepp, A.; Habib, F.A.; Heinemann, T.; Irman, A.; Karsch, S.; Kirwan, G.; et al. Fundamentals and Applications of Hybrid LWFA-PWFA. *Appl. Sci.* **2019**, *9*, 2626. [CrossRef]
11. Weikum, M.K.; Akhter, T.; Alesini, P.D.; Alexandrova, A.S.; Anania, M.P.; Andreev, N.E.; Andriyash, I.; Aschikhin, A.; Assmann, R.W.; Audet, T.; et al. EuPRAXIA—A compact, cost-efficient particle and radiation source. *AIP Conf. Proc.* **2019**, *2160*, 040012. [CrossRef]
12. Weikum, M.K.; Akhter, T.; Alesini, D.; Alexandrova, A.S.; Anania, M.P.; Andreev, N.E.; Andriyash, I.A.; Aschikhin, A.; Assmann, R.W.; Audet, T.; et al. Status of the Horizon 2020 EuPRAXIA conceptual design study. *J. Phys. Conf. Ser.* **2019**, *1350*, 012059.

13. Assmann, R.W.; Weikum, M.K.; Akhter, T.; Alesini, D.; Alexandrova, A.S.; Anania, M.P.; Andreev, N.E.; Andriyash, I.; Artioli, M.; Aschikhin, A.; et al. EuPRAXIA Conceptual Design Report. *Eur. Phys. J. Spec. Top.* **2020**, *229*, 3675–4284; Erratum in *Eur. Phys. J. Spec. Top.* **2020**, *229*, 4285–4287. [CrossRef]
14. Tomassini, P.; Nicola, S.D.; Labate, L.; Londrillo, P.; Fedele, R.; Terzani, D.; Gizzi, L.A. The resonant multi-pulse ionization injection. *Phys. Plasmas* **2017**, *24*, 103120. [CrossRef]
15. Fiore, G.; Fedele, R.; de Angelis, U. The slingshot effect: A possible new laser-driven high energy acceleration mechanism for electrons. *Phys. Plasmas* **2014**, *21*, 113105. [CrossRef]
16. Akhiezer, A.I.; Polovin, R.V. Theory of wave motion of an electron plasma. *Sov. Phys. JETP* **1956**, *3*, 696. [CrossRef]
17. Gorbunov, L.M.; Kirsanov, V.I. Excitation of plasma waves by an electromagnetic wave packet. *Sov. Phys. JETP* **1987**, *66*, 290.
18. Rosenzweig, J.; Breizman, B.; Katsouleas, T.; Su, J. Acceleration and focusing of electrons in two-dimensional nonlinear plasma wake fields. *Phys. Rev.* **1991**, *A44*, R6189.
19. Mora, P.; Antonsen, T.M. Electron cavitation and acceleration in the wake of an ultraintense, self-focused laser pulse. *Phys. Rev.* **1996**, *E53*, R2068(R). [CrossRef]
20. Pukhov, A.; Meyer-ter-Vehn, J. Laser wake field acceleration: The highly non-linear broken-wave regime. *Appl. Phys.* **2002**, *B74*, 355–361. [CrossRef]
21. Kostyukov, I.; Pukhov, A.; Kiselev, S. Phenomenological theory of laser-plasma interaction in 'bubble' regime. *Phys. Plasmas* **2004**, *11*, 5256. [CrossRef]
22. Lu, W.; Huang, C.; Zhou, M.; Mori, W.; Katsouleas, T. Nonlinear theory for relativistic plasma wakefields in the blowout regime. *Phys. Rev. Lett.* **2006**, *96*, 165002. [CrossRef]
23. Lu, W.; Huang, C.; Zhou, M.; Tzoufras, M.; Tsung, F.S.; Mori, W.B.; Katsouleas, T. A nonlinear theory for multidimensional relativistic plasma wave wakefields. *Phys. Plasmas* **2006**, 13, 056709. [CrossRef]
24. Maslov, V.I.; Svystun, O.M.; Onishchenko, I.N.; Tkachenko, V.I. Dynamics of electron bunches at the laser–plasma interaction in the bubble regime. *Nucl. Instrum. Meth. Phys. Res.* **2016**, *A829*, 422. [CrossRef]
25. Fiore, G.; Nicola, S.D. A simple model of the slingshot effect. *Phys Rev. Acc. Beams* **2016**, *19*, 071302. [CrossRef]
26. Fiore, G.; Nicola, S.D. A "slingshot" laser-driven acceleration mechanism of plasma electrons. *Nucl. Instrum. Meth. Phys. Res.* **2016**, *A829*, 104–108. [CrossRef]
27. Fiore, G.; Catelan, P. On cold diluted plasmas hit by short laser pulses. *Nucl. Instrum. Meth. Phys. Res.* **2018**, *A 909*, 41–45. [CrossRef]
28. Fiore, G.; Akhter, T.; Nicola, S.D.; Fedele, R.; Jovanović, D. On the impact of short laser pulses on cold diluted plasmas. 2022, *in preparation*. [CrossRef]
29. Fiore, G. The time-dependent harmonic oscillator revisited. *arXiv* **2022**, arXiv:2205.01781.
30. Fiore, G. On plane-wave relativistic electrodynamics in plasmas and in vacuum. *J. Phys. A Math. Theory* **2014**, *47*, 225501.
31. Fiore, G. Travelling waves and a fruitful 'time' reparametrization in relativistic electrodynamics. *J. Phys. A Math. Theory* **2018**, *51*, 085203. [CrossRef]
32. Fiore, G. On plane waves in Diluted Relativistic Cold Plasmas. *Acta Appl. Math.* **2014**, *132*, 261. [CrossRef]
33. Fiore, G. On very short and intense laser-plasma interactions. *Ricerche Mat.* **2016**, *65*, 491–503. [CrossRef]
34. Fiore, G.; Catelan, P. Travelling waves and light-front approach in relativistic electrodynamics. *Ricerche Mat.* **2019**, *68* , 341–357. [CrossRef]
35. Fiore, G. Light-front approach to relativistic electrodynamics. *J. Phys. Conf. Ser.* **2021**, *1730*, 012106. [CrossRef]
36. Dawson, J.D. Nonlinear electron oscillations in a cold plasma. *Phys. Rev.* **1959**, *113*, 383. [CrossRef]
37. Jovanovic, D.; Fedele, R.; Belic, M.; Nicola, S.D. Adiabatic Vlasov theory of ultrastrong femtosecond laser pulse propagation in plasma. The scaling of ultrarelativistic quasi-stationary states: Spikes, peakons, and bubbles. *Phys. Plasmas* **2019**. *26*. 123104. [CrossRef]
38. Yoshizawa, T. *Stability Theory by Liapunov's Second Method*; Mathematical Society of Japan: Tokyo, Japan, 1966; 223p. [CrossRef]
39. Hosokai, T.; Kinoshita, K.; Watanabe, T.; Yoshii, K.; Ueda, T.; Zhidokov, A.; Uesaka, M. Supersonic gas jet target for generation of relativistic electrons with 12-TW 50-fs laser pulse. In Proceedings of the 8th European Conference, EPAC 2002, Paris, France, 3–7 June 2002; pp. 981–983.
40. Veisz, L.; Buck, A.; Nicolai, M.; Schmid, K.; Sears, C.M.S.; Sävert, A.; Mikhailova, J.M.; Krausz, F.; Kaluza, M.C. Complete characterization of laser wakefield acceleration. In Proceedings of the Volume 8079, Laser Acceleration of Electrons, Protons, and Ions; and Medical Applications of Laser-Generated Secondary Sources of Radiation and Particles, Prague, Czech Republic, 18–21 April 2011.